doi:10.1093/brain/awu057 Brain 2014: 137; 1496–1513 | 1496

BRAIN
A JOURNAL OF NEUROLOGY

Accumulation of oligomer-prone α-synuclein exacerbates synaptic and neuronal degeneration *in vivo*

Edward Rockenstein,[1] Silke Nuber,[1] Cassia R. Overk,[1] Kiren Ubhi,[1] Michael Mante,[1] Christina Patrick,[1] Anthony Adame,[1] Margarita Trejo-Morales,[1] Juan Gerez,[2] Paola Picotti,[2] Poul H. Jensen,[3] Silvia Campioni,[4] Roland Riek,[4] Jürgen Winkler,[5] Fred H. Gage,[6] Beate Winner[7] and Eliezer Masliah[1,8]

1 Department of Neurosciences, University of California San Diego, La Jolla, CA, USA
2 Institute of Biochemistry, ETH Zurich, Switzerland
3 Institute of Medical Biochemistry, University of Aarhus, Denmark
4 Lab. F. Physikalische Chemie, ETH Zurich, Switzerland
5 Department of Molecular Neurology, University Hospital Erlangen, Schwabachanlage 6, 91054 Erlangen, Germany
6 Laboratory of Genetics, The Salk Institute for Biological Studies, 10010 North Torrey Pines Road, La Jolla, CA 92037, USA
7 IZKF Junior Research Group III, Nikolaus-Fiebiger-Zentrum, FAU Erlangen-Nürnberg, Erlangen, Germany
8 Department of Pathology, University of California San Diego, La Jolla, CA 92039, USA

Correspondence to: Dr Eliezer Masliah,
Department of Neurosciences,
University of California,
San Diego, La Jolla,
CA 92093-0624 USA.
E-mail: emasliah@ucsd.edu

In Parkinson's disease and dementia with Lewy bodies, α-synuclein aggregates to form oligomers and fibrils; however, the precise nature of the toxic α-synuclein species remains unclear. A number of synthetic α-synuclein mutations were recently created (E57K and E35K) that produce species of α-synuclein that preferentially form oligomers and increase α-synuclein-mediated toxicity. We have shown that acute lentiviral expression of α-synuclein E57K leads to the degeneration of dopaminergic neurons; however, the effects of chronic expression of oligomer-prone α-synuclein in synapses throughout the brain have not been investigated. Such a study could provide insight into the possible mechanism(s) through which accumulation of α-synuclein oligomers in the synapse leads to neurodegeneration. For this purpose, we compared the patterns of neurodegeneration and synaptic damage between a newly generated mThy-1 α-synuclein E57K transgenic mouse model that is prone to forming oligomers and the mThy-1 α-synuclein wild-type mouse model (Line 61), which accumulates various forms of α-synuclein. Three lines of α-synuclein E57K (Lines 9, 16 and 54) were generated and compared with the wild-type. The α-synuclein E57K Lines 9 and 16 were higher expressings of α-synuclein, similar to α-synuclein wild-type Line 61, and Line 54 was a low expressing of α-synuclein compared to Line 61. By immunoblot analysis, the higher-expressing α-synuclein E57K transgenic mice showed abundant oligomeric, but not fibrillar, α-synuclein whereas lower-expressing mice accumulated monomeric α-synuclein. Monomers, oligomers, and fibrils were present in α-synuclein wild-type Line 61. Immunohistochemical and ultrastructural analyses demonstrated that α-synuclein accumulated in the synapses but not in the neuronal cells bodies, which was different from the α-synuclein wild-type Line 61, which accumulates α-synuclein in the soma. Compared to non-transgenic and lower-expressing mice, the higher-expressing α-synuclein E57K mice displayed synaptic and dendritic loss, reduced levels of synapsin 1 and synaptic vesicles, and behavioural deficits. Similar alterations, but to a lesser extent, were seen in the α-synu-

Received August 1, 2013. Revised January 23, 2014. Accepted January 27, 2014. Advance Access publication March 24, 2014
© The Author (2014). Published by Oxford University Press on behalf of the Guarantors of Brain. All rights reserved.
For Permissions, please email: journals.permissions@oup.com

clein wild-type mice. Moreover, although the oligomer-prone α-synuclein mice displayed neurodegeneration in the frontal cortex and hippocampus, the α-synuclein wild-type only displayed neuronal loss in the hippocampus. These results support the hypothesis that accumulating oligomeric α-synuclein may mediate early synaptic pathology in Parkinson's disease and dementia with Lewy bodies by disrupting synaptic vesicles. This oligomer-prone model might be useful for evaluating therapies directed at oligomer reduction.

Keywords: α-synuclein; transgenic; oligomer; Parkinson's disease; synaptic vesicles

Abbreviation: SNARE = soluble NSF attachment protein receptor

Introduction

α-Synucleinopathies are a heterogeneous group of neurodegenerative disorders characterized by widespread neurodegeneration (Hardy, 2010) and by abnormal accumulation of α-synuclein. α-Synuclein is a 14 kDa (Weinreb *et al.*, 1996) synaptic protein (Iwai *et al.*, 1995) involved in vesicular release (Burre *et al.*, 2010). Pathological accumulation of α-synuclein occurs predominantly in neuronal cells and synapses, as observed in Parkinson's disease and dementia with Lewy bodies (Spillantini *et al.*, 1997; Takeda *et al.*, 1998), or in glial cells, as observed in multiple system atrophy (Papp and Lantos, 1994; Wakabayashi *et al.*, 1998). There is great interest in what causes α-synuclein to undergo conformational changes to form oligomers, protofibrils and fibrils, which accumulate in cells (Uversky *et al.*, 2001; Tsigelny *et al.*, 2012). The relative toxic contribution of the different α-synuclein arrays, namely monomers, oligomers and fibrils, has been scrutinized. Although the precise identification of the toxic α-synuclein species remains unclear, clues to its identity come from familial forms of α-synucleinopathy where mutated forms of α-synuclein (A53T, E46K) (Polymeropoulos *et al.*, 1997) form oligomers faster than wild-type α-synuclein (Conway *et al.*, 1998). Likewise, in sporadic forms of α-synucleinopathies, post-translational modifications including C-terminus cleavage (Sung *et al.*, 2005), oxidation, nitration (Hodara *et al.*, 2004) and phosphorylation (Fujiwara *et al.*, 2002) might contribute to oligomerization, polymerization and toxicity (Paleologou *et al.*, 2010).

In facilitating our ability to study the oligomeric forms of α-synuclein and to assess its toxic characteristics, we previously generated variants of α-synuclein bearing synthetic mutations (E35K and E57K) designed to disrupt α-synuclein-specific salt bridges and thereby alter the structure of α-synuclein. These mutations resulted in α-synuclein species that specifically formed oligomers but not fibrils (Winner *et al.*, 2011) and when delivered into the substantia nigra by way of lentiviral vector injection, led to dopaminergic cell loss. The viral vector injection system provides information about the acute local effects of α-synuclein oligomers; however, the effects of chronic and more widespread α-synuclein E57K expression in other areas of the brain associated with dementia with Lewy bodies and the other α-synucleinopathies remain unexamined. A model with these characteristics could provide insight into the possible mechanism(s) through which accumulation of α-synuclein oligomers in the synapse leads to neurodegeneration.

In this context, we generated oligomer-prone novel transgenic mouse lines expressing higher- and lower-levels of human α-synuclein bearing the synthetic α-synuclein E57K mutation under the control of the neuronal mThy-1 promoter, and then we compared them to α-synuclein wild-type mice. α-Synuclein E57K mice displayed synaptic and dendritic loss, reduced levels of synapsin 1 and synaptic vesicles, and behavioural deficits. Similar alterations were seen in α-synuclein wild-type mice; however, although oligomer-prone α-synuclein mice displayed neurodegeneration in the frontal cortex and hippocampus, α-synuclein wild-type mice only displayed neuronal loss in the hippocampus. These results support the hypothesis that accumulating oligomeric α-synuclein may mediate early neurodegenerative changes by disrupting synaptic vesicles. This oligomer-prone model might be useful for evaluating therapies directed at oligomer reduction.

Materials and methods

Generation of mThy-1 human α-synuclein E57K transgenic mice

The University of California at San Diego's animal subjects committee approved all experiments. Mice expressing human (h)α-synuclein bearing the oligomer-prone E57K mutation under the neuronal mThy-1 promoter cassette (provided by Dr H. van der Putten, Ciba-Geigy, Basel, Switzerland) were generated. The α-synuclein E57K variant was constructed by site-directed mutagenesis (QuikChange kit; Stratagene) and confirmed by DNA sequencing (Winner *et al.*, 2011). The α-synuclein E57K complementary DNA fragment was ligated into pCRII (Invitrogen), sequenced for accuracy, inserted into the mThy-1 expression cassette between exons 2 and 4, purified, and microinjected into single-cell embryos (C57BL/6 × DBA/2F1) (Rockenstein *et al.*, 2002). Genomic DNA, extracted from tail biopsies, was analysed by PCR amplification (Rockenstein *et al.*, 1995; Masliah *et al.*, 2000). Heterozygous α-synuclein E57K mice were crossed with wild-type (DBA) mice to generate transgenic and non-transgenic littermates. Lines expressing lower (Line 54) and higher (Lines 9 and 16) levels of α-synuclein were selected for analysis compared to our previously described mThy-1 α-synuclein wild-type Line 61 (Rockenstein *et al.*, 2002), which accumulates various species of α-synuclein accompanied by axonal pathology, dopaminergic and behaviour deficits (Games *et al.*, 2013).

Behavioural analysis

Context-dependent learning in an open field data were collected using a Kinder SmartFrame Cage Rack Station activity monitor system (Kinder Scientific), in 3D space using a 7 × 15 beam configuration.

Data collection began when an animal was placed in the test chamber. Animals were evaluated for 10 min for three consecutive days, given a 2-day dishabituation period, followed by a fourth trial (Chen *et al.*, 2012; Sanchez *et al.*, 2012).

Tissue preparation

After behavioural analysis, mice were sacrificed following NIH guidelines. The right hemi-brain was post-fixed for 48 h in 4% phosphate-buffered paraformaldehyde (pH 7.4) at 4°C and sagittal sectioned Vibratome 2000 (40 μm; Leica). The left hemi-brain was snap-frozen and stored at −70°C.

Real-time polymerase chain reaction

RNA was extracted from mice in triplicate using the RNeasy® kit (QIAGEN) (Rockenstein *et al.*, 2002), and quantified by spectrophotometer readings. For complementary DNA synthesis, 1 μg total RNA was reverse transcribed using iScript™ cDNA Synthesis kit (Bio-Rad). Real-time PCR experiments were performed using the iQ™5 Detection System (Bio-Rad). Amplification was performed on complementary DNA equivalent to 25 ng total RNA with 1 × iQ™ SYBR®Green Supermix (Bio-Rad). Template PCR reactions were performed in triplicate and run in duplicate using the following PCR cycling parameters: 50°C for 2 min, 95°C for 10 min, and 40 cycles of 94°C for 15 s, 60°C for 1 min before a dissociation protocol to verify the presence of a single product for each amplicon. The amount of complementary DNA was calculated by the comparative threshold cycle method and expressed using mouse actin as an internal control.

Immunohistochemical analysis

Analysis of α-synuclein accumulation was performed using free-floating, blind-coded sections (Ubhi *et al.*, 2010; Masliah *et al.*, 2011). Sections were incubated overnight at 4°C with antibodies against total α-synuclein (1:500, affinity purified rabbit polyclonal, Millipore) (Masliah *et al.*, 2000), human α-synuclein (LB509, mouse monoclonal), and pSer129 α-synuclein (mouse monoclonal, Wako laboratories), followed by biotin-tagged anti-rabbit or anti-mouse IgG1 (1:100, Vector Laboratories, Inc.) secondary antibodies, Avidin D-HRP (1:200, ABC Elite, Vector), and visualized with diaminobenzidine. Sections were scanned with a digital Olympus bright field digital microscope (BX41).

Neurodegenerative pathology was observed using sections immunolabelled overnight with antibodies against the dendritic marker microtubule-associated protein 2 (MAP2; 1:500, Millipore), neuronal marker NeuN (1:500, Millipore), astroglial marker glial fibrillary acidic protein (GFAP, 1:1000, Millipore), and synaptic marker synaptophysin (SY38, 1:500, Millipore) (Ubhi *et al.*, 2010; Masliah *et al.*, 2011). Sections reacted with antibodies against NeuN or GFAP were incubated with secondary antibodies, Avidin D-HRP, and visualized with diaminobenzidine. Sections reacted with antibodies against MAP2 and synaptophysin were visualized with FITC-tagged secondary antibody or the Tyramide Signal Amplification™ Direct (Red) system (1:100, NEN Life Sciences), respectively, mounted under glass coverslips with anti-fading media (Vector Laboratories), and imaged with the laser scanning confocal microscope (MRC1024, Bio-Rad).

The numbers of NeuN-immunoreactive neurons were estimated using unbiased stereological methods (Overk *et al.*, 2009). Hemi-sections containing the neocortex, hippocampus and striatum were outlined using an Olympus BX51 microscope running StereoInvestigator 8.21.1 software (Micro-BrightField). Grid sizes for the striatum, frontal cortex, and hippocampal CA3 pyramidal layer were: 900 × 900, 800 × 800, and 300 × 300 μm, respectively, and the counting frames were 40 × 40, 30 × 30, and 50 × 50 μm, respectively. The average coefficient of error for each region was 0.9. Sections were analysed using a 100 × 1.4 PlanApo oil-immersion objective. A 5-μm high disector, allowed for 2 μm top and bottom guard-zones.

Double immunolabelling and fluorescence co-labelling

To determine the co-localization between α-synuclein and synaptic markers, double-labelling experiments were performed (Masliah *et al.*, 2011). Sections were immunolabelled with antibodies against human α-synuclein (SYN211) and synaptophysin (SY38, Millipore). To compare the proportion of synapses containing synapsin 1 in non-transgenic versus α-synuclein E57K mice and α-synuclein wild-type mice, double-labelling experiments were performed with antibodies against synapsin 1 and synaptophysin (SY38, Millipore). All sections were processed simultaneously, and experiments were performed in triplicate. The synaptophysin-immunoreactive terminals were detected with Tyramide Red (NEN Life Sciences), whereas SYN211 and synapsin 1 were detected with FITC-tagged antibodies (1:75, Vector). Sections were imaged with a Zeiss × 63 1.4 objective on an Axiovert 35 microscope (Zeiss) with an attached MRC1024 laser scanning confocal microscope system (Bio-Rad) (Masliah *et al.*, 2011). Paired optical sections were analysed with ImageJ co-localization colour map software to determine the per cent of synaptophysin-positive terminals containing α-synuclein- or synapsin -1-immunoreactivity. For each mouse, ~20 digital images, each containing 700 synapses on average, were analysed. Per cent neuropil was calculated based on area of intensity above threshold divided by the geometric area.

Tissue fractionation, immunoblot analysis and size exclusion chromatography

Conventional immunoblot

The distribution and levels of α-synuclein in mouse brains were analysed using lysate that were extracted and fractioned into soluble and insoluble fractions by ultracentrifugation (Masliah *et al.*, 2011). Protein (20 μg/lane) was loaded onto 4–12% SDS/PAGE gels and blotted onto polyvinylidene difluoride membranes, incubated with rabbit polyclonal anti-α-synuclein (1:1000; Millipore) or mouse monoclonal α-synuclein antibody (1:1000; BD), followed by HRP-tagged secondary antibodies (1:5000; Santa Cruz Biotechnology). Bands were visualized by enhanced chemiluminescence (PerkinElmer) and analysed with a quantitative Versadoc XL imaging apparatus (Bio-Rad). β-Actin (1:3000) was the loading control.

Sequential extraction

Oligomers were evaluated using additional immunoblot analysis of protein following three sequential extractions to generate Tris-buffered saline (TBS)-, TBST-, and urea-soluble fractions (Tofaris *et al.*, 2006). Protein extracts were run on 4–12% Bis-Tris gels (Invitrogen) and electroblotted onto nitrocellulose membranes (Millipore). Membranes were fixed in 0.4% paraformaldehyde for 30 min (Lee and Kamitani, 2011), washed in PBS, and blocked for 30 min in PBS Tween (PBS with 0.2% Tween-20, and 5% bovine serum albumin), followed by

incubation with either SYN211 (1:600; Sigma) or human- and rodent-specific antibody SYN1 (1:1000; BD Bioscience in PBS Tween containing 5% bovine serum albumin) overnight. After washing with PBS Tween, membranes were probed with anti-mouse secondary antibodies (1:5000, American Qualex), normalized as above and quantified (Nuber *et al.*, 2008).

Native gel electrophoresis was conducted on 12% Tris-glycine gels with native (SDS-free) running and sample loading buffer (Invitrogen) (Fauvet *et al.*, 2012).

Sequential homogenates were further fractionated by size exclusion chromatography using a S200 10/300 GL column (GE Healthcare), previously equilibrated in TBS + buffer with 0.05% (w/v) sodium azide. Elution was performed at 0.5 ml/min monitoring UV signals at 280 nm and 260 nm. Fractions of 0.5 ml were collected during elution, starting at 6 ml (just before the void volume) and ending at 22 ml (close to the end of the column). Aliquots of the eluted fractions were then used for SDS-PAGE and western blot analyses. LB509 from Abcam was used as primary antibody.

Cases with dementia with Lewy bodies

For comparison with the sequential immunoblot assay in the α-synuclein mice, frozen samples from the right hemisphere from six dementia with Lewy bodies cases were obtained from patients evaluated neurologically and psychometrically at the Alzheimer Disease Research Centre, University of California, San Diego (Hansen, 1997). Control cases were obtained from the German Brain Bank. The diagnosis was based on the clinical presentation of dementia and the pathological findings of Lewy bodies were detected with antibodies against α-synuclein, as recommended (McKeith *et al.*, 1996). Tissue was sequentially extracted and 25 μg of TBS and urea extracts used for immunoblot studies, as described above (Nuber *et al.*, 2013).

Fibril assembly

For generation of a dot blot standard, fibrils were prepared using 1 mg/ml α-synuclein monomer in assembly buffer (50 mM Tris, 100 mM NaCl, pH 7.0) and agitated (37°C; 1000 rpm). Reaction was stopped after 3 days, diluted with PBS (10 μM final concentration) and stored at −20°C. A short sonication with a tip sonicator (Fisher Scientific) increased the dissociation of small oligomers to generate 'seeds'.

Dot blot analysis

Formation of α-synuclein oligomers was determined using dot blot measurements with the A11 antibody (1:4000; BioSource) (Kayed *et al.*, 2003). Duplicate cytosolic or hippocampal Triton™ X-100 membrane fractions (8 μg) were spotted on a polyvinylidene difluoride membrane, blocked for 30 min with 5% bovine serum albumin in PBS Tween, incubated with A11 for 1.5 h at room temperature, and treated with HRP-conjugated anti-rabbit IgG for 45 min. Bands were visualized with enhanced chemiluminescence, and analysed using Image Quant Software (Amersham Bioscience).

Electron microscopy and immunogold analysis

Vibratome sections from the non-transgenic and α-synuclein E57K mice (Line 16) were post-fixed in 1% glutaraldehyde, treated with osmium tetroxide, embedded in Epon® araldite and sectioned with the ultramicrotome (Leica) (Masliah *et al.*, 2011). Grids were analysed with a Zeiss OM10 electron microscope (Rockenstein *et al.*, 2001). These same serial sections were used for analysis of synaptic vesicle counts (Applegate and Landfield, 1988). Approximately 100 terminals and 2500 vesicles were analysed per animal. Immunogold-labelled sections were mounted on nickel grids, etched and incubated with the LB509 antibody (1:50) and labelled with 10 nm Aurion ImmunoGold particles (1:50, Electron Microscopy Sciences) with silver enhancement. Electron micrographs (×25 000 magnification) were obtained.

Statistical analysis

All analyses used GraphPad Prism (version 5.0). Differences among means were assessed by one-way ANOVA with Dunnett's *post hoc* test when compared to non-transgenic and by Tukey-Kramer when comparing transgenic groups. Two-way ANOVA with repeated measures followed by a Bonferroni multiple comparisons *post hoc* test was used for analysing the interactions between groups and time. The null hypothesis was rejected at the 0.05 level.

Results

Characterization and comparison of messenger RNA and protein expression in transgenic mouse lines expressing the α-synuclein E57K mutation versus wild-type α-synuclein

To investigate the effects of chronic widespread expression of oligomer-prone α-synuclein, we generated novel transgenic mouse lines (Lines 9, 16 and 54) expressing the α-synuclein E57K mutation under the control of the neuronal mThy-1 promoter (Fig. 1A), and analysed them with mThy-1 α-synuclein wild-type Line 61 for expression of α-synuclein at the messenger RNA (Fig. 1B) and protein levels (Fig. 1C). Quantitative PCR analysis of messenger RNA isolated from brain tissue demonstrated that α-synuclein E57K Lines 9 and 16 were higher-expressing lines, similar to α-synuclein wild-type Line 61 (Fig. 1B) (Rockenstein *et al.*, 2002), whereas α-synuclein E57K Line 54 was a low-expressing line producing a fifth of the Line 61 expression (Fig. 1B). Consistent with the quantitative PCR results, immunoblot analysis demonstrated that α-synuclein E57K Lines 9 and 16 and α-synuclein wild-type Line 61 expressed significantly higher levels of α-synuclein compared to non-transgenic mice (Fig. 1C–F). α-Synuclein was primarily found in the cytosolic fraction, and the most abundant band was detected at 14 kDa, corresponding to monomeric α-synuclein (Fig. 1C and D). Other bands between 28 and 62 kDa were found in the Lines 9 and 16 and, to a lesser extent, in Line 61. In the membrane fraction, the 14 kDa band was detected to a significantly greater extent in α-synuclein E57K Lines 9 and 16 and α-synuclein wild-type Line 61, but not in Line 54 (Fig. 1E and F). Compared to the α-synuclein E57K lines, the α-synuclein wild-type mice displayed a prominent band at 28 kDa in the membrane fraction (Fig. 1E). Levels of α-synuclein protein in α-synuclein E57K Lines 9 and 16 were comparable to those observed in α-synuclein wild-type mice (Line 61; Fig. 1E and F).

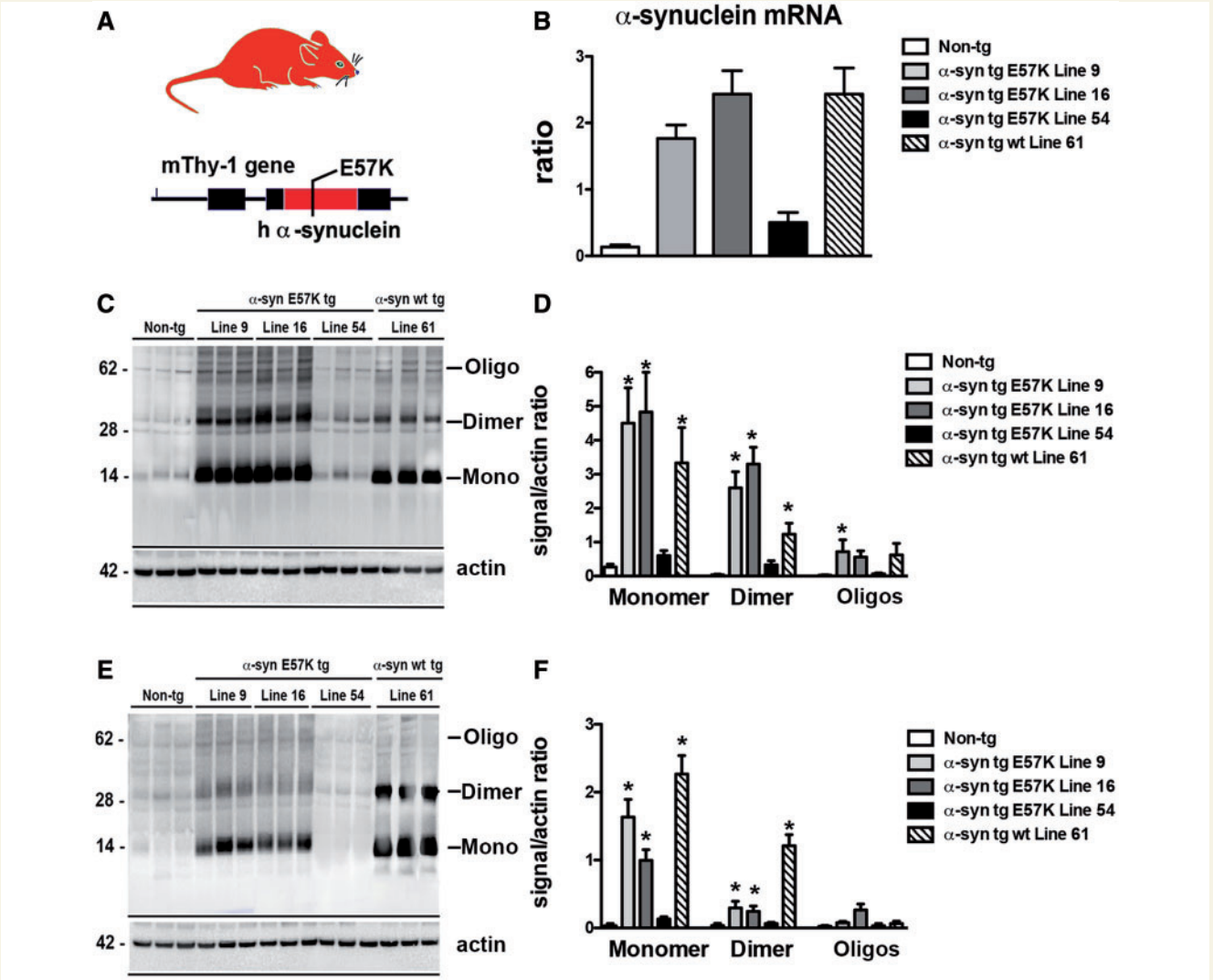

Figure 1 Generation of transgenic mice expressing the synthetic α-synuclein mutation E57K under the mThy-1 promoter. (**A**) Diagram of the mThy-1 construct. (**B**) Levels of α-synuclein messenger RNA expressed as a ratio to the housekeeping gene *Gadph* in non-transgenic and α-synuclein E57K Lines 9, 16, and 54, showing that Line 54 had 0.2 of the expression compared to α-synuclein E57K Line 9 and 16 and α-synuclein wild-type Line 61 transgenic mice. (**C**) Representative western blot (SDS) and (**D**) analysis of the levels of α-synuclein in the cytosolic fractions showing that Lines 9 and 16 were higher expressers of α-synuclein monomers and dimers, which was to a similar extent as Line 61. **(E)** Representative western blot (SDS) and (**F**) analysis of levels of monomer, dimer, and oligomer α-synuclein immunoreactivity in the membrane-bound fractions. Across all lines monomeric α-synuclein (14 kDa) was present to a greater extent in the cytosolic fraction compared to the membrane fraction. For analysis, six non-transgenic and six mThy-1 α-synuclein E57K transgenic mice (3–4 months old) from each line were used. $^*P < 0.05$ when compared to non-transgenic control using one way ANOVA with Dunnet's *post hoc* test. Tg = transgenic; wt = wild-type.

Characterization of α-synuclein aggregates in the α-synuclein E57K transgenic mouse lines

To investigate the formation of α-synuclein aggregates in the α-synuclein E57K mice, we performed sequential extraction procedures with detergent-containing buffers yielding three main extracts. The first extract was enriched in TBS-soluble cytosolic proteins, the second extract contained Triton^{TM} X-100-soluble membrane and organelle proteins, and the third extract contained SDS/urea-soluble proteins, including integral membrane proteins and cytoskeletal filaments (Schindler *et al.*, 2006). In urea-treated extracts, complex α-synuclein aggregates typically solubilize as a high-molecular weight band and its monomer (Culvenor *et al.*, 1999; Campbell *et al.*, 2001; Kahle *et al.*, 2001; Liu *et al.*, 2005; Tong *et al.*, 2010) (Fig. 2A). Western blot analyses of the TBS-soluble extracts of hippocampi showed a similar band at ~14 kDa in Lines 9, 16 and 61 (Fig. 2A). Incubation with the human-specific anti-α-synuclein with the urea-soluble fraction showed a specific band running at ~70 kDa molecular weight

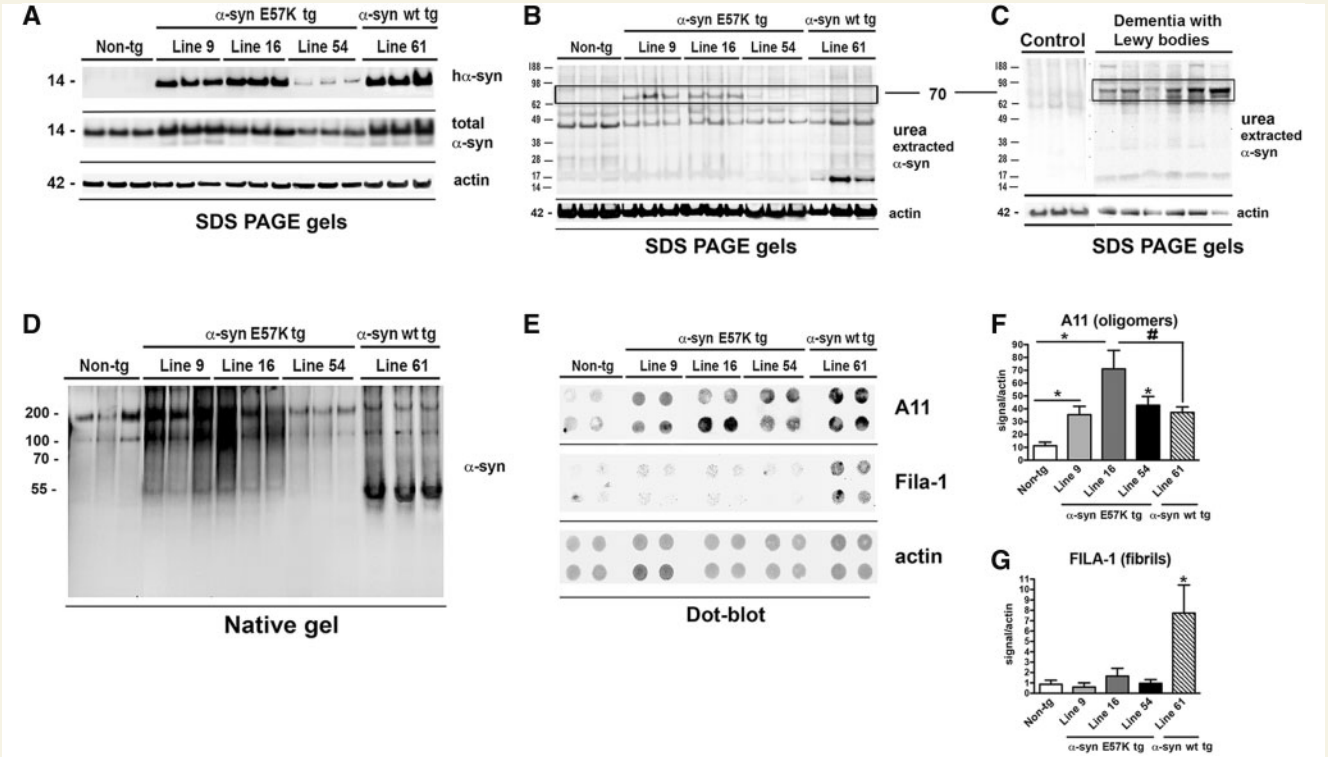

Figure 2 Immunoblot analysis of α-synuclein oligomers in the α-synuclein E57K and α-synuclein wild-type transgenic mice. (**A**) Western blot evaluation indicated that all transgenic lines were positive for human α-synuclein, which was absent in the non-transgenic mice; whereas all mouse lines were positive for total α-synuclein. (**B**) After urea extraction, α-synuclein E57K Lines 9 and 16 had bands ~70 kDa (pentamers), which were not present in the lower-expressing α-synuclein E57K Line 54, α-synuclein wild-type or non-transgenic mice, but which were present (**C**) in frontal cortex from controls and cases with dementia with Lewy bodies. (**D**) Analysis of α-synuclein in native gel reveals a faint band at ~55 kDa for Lines 9, 16, and 54; a dense smear between 70 and 200 kDa was most prominent in Lines 9 and 16. In the α-synuclein wild-type animal line, there was a prominent band at ~55 kDa and less smearing between 70 and 200 kDa. (**E**) Representative image of the dot blot analysis with the A11 and FILA-1 antibodies using Triton™ X-100 membrane-extracted fraction indicated that α-synuclein oligomers (**F**) were present in all α-synuclein E57K transgenic lines, and Line 61, albeit to a lesser extent than in Line 16. (**G**) Only Line 61 had significant levels of fibrils above non-transgenic background. Seeded and fibrillized dose responses of recombinant α-synuclein protein were generated for qualitative concentration analysis. For analysis, four non-transgenic and six transgenic mice (3–4 months old) from each line were used. Tg = transgenic; wt = wild-type * = p-value <0.05 compared to non-tg; # = p-value < 0.05 compared to Line 61.

marker in α-synuclein E57K Lines 9 and 16 mice, consistent with pentamer α-synuclein conformer (Fig. 2B), which was also present in cases with dementia with Lewy bodies (Fig. 2C). Although urea-soluble fraction from α-synuclein wild-type Line 61 mice had a strong band at ~14 kDa (Fig. 2B), it was faint in the α-synuclein E57K, non-transgenic lines, and dementia with Lewy body cases (Fig. 2C). Immunoblot analysis of α-synuclein in native gels was consistent with previous studies (Fauvet *et al.*, 2012), which showed a faint band at ~55 kDa for Lines 9, 16 and 54, and a dense smear was most prominent in Lines 9 and 16 between 70–200 kDa. In the α-synuclein wild-type transgenic line, there was a prominent band at ~55 kDa, but a less prominent smearing between 70–200 kDa (Fig. 2D). In agreement with the immunoblot analysis, dot blot analysis with the antibody against oligomers (A11) showed the presence of abundant immunoreactive material in the TBS-soluble fraction in Lines 9, 16, 54 and 61 transgenic mice, but not in the non-transgenic controls (Fig. 2E and F). Although Line 61 had significantly less oligomeric protein compared with Line 16 (Fig. 2E and F), analysis for the presence of fibrils (FILA-1) indicated that only Line 61 had a significant level compared to non-transgenic background (Fig. 2E and G). Size exclusion chromatography using homogenates that were biochemically fractionated into soluble (Fig. 3A and B) and urea (Fig. 3C and D) fractions further confirmed that α-synuclein E57K mice were more prone to form oligomeric α-synuclein compared to the α-synuclein wild-type line.

Patterns of α-synuclein immunoreactivity and distribution in α-synuclein E57K transgenic compared with α-synuclein wild-type transgenic mice

To analyse the anatomical distribution of α-synuclein in the α-synuclein E57K mice, sections were immunolabelled with antibodies against total α-synuclein. As expected, in the non-transgenic mice the antibody against total α-synuclein reacted mildly with fine granular structures in the neuropil throughout the CNS,

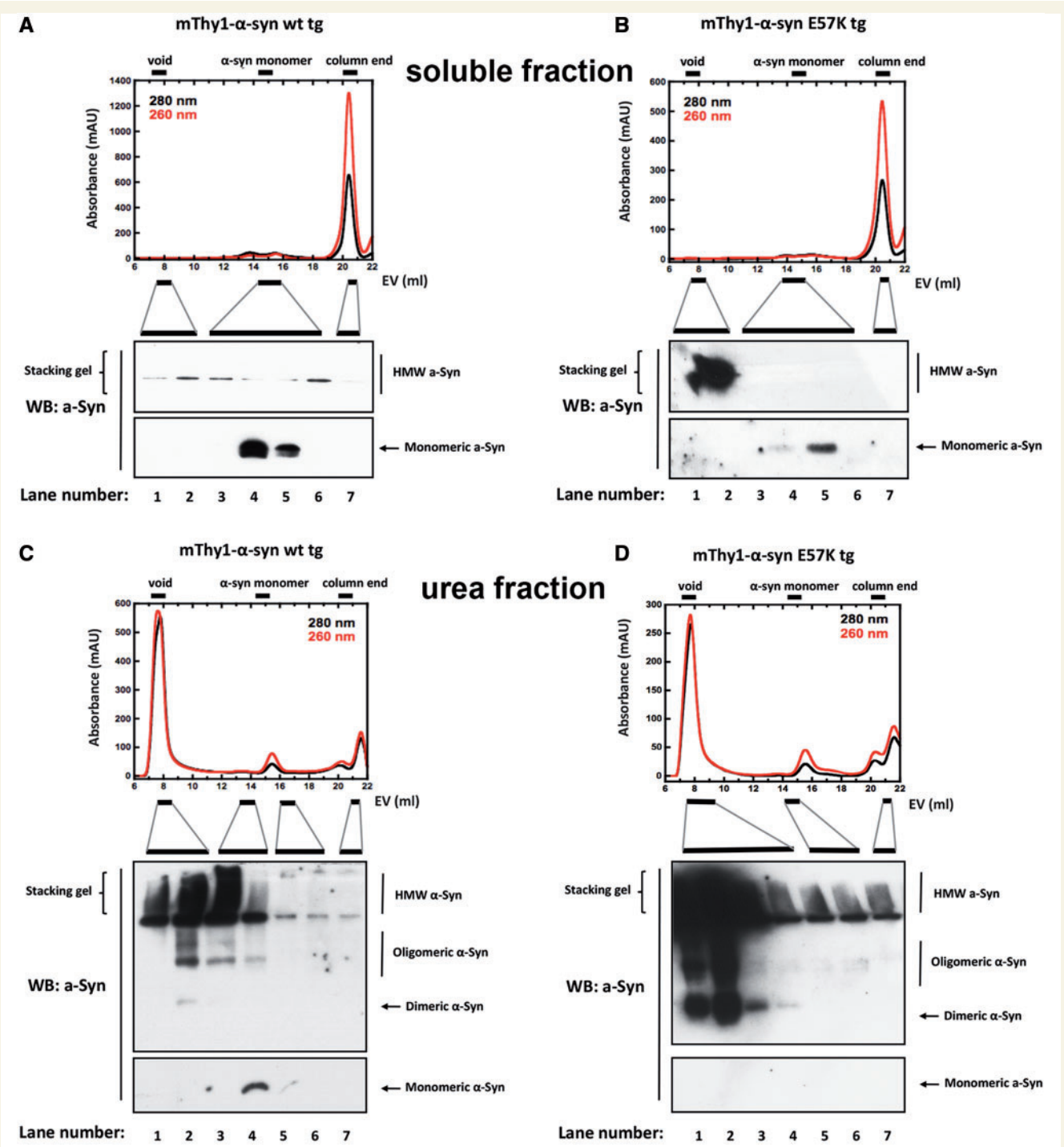

Figure 3 Separation of oligomeric and monomeric species in extracts of wild-type and E57K transgenic mice using size exclusion chromatography-profiles (*top*) before western blot (*bottom*). (**A**) α-Synuclein extracted from α-synuclein wild-type mice with TBS + buffer was found as monomers and small oligomers (lanes 4 and 5). (**B**) α-Synuclein E57K-transgenic mice brain extracts contained monomeric α-synuclein (lane 5 *bottom*) and oligomers with a molecular weight >200 kDa, which elute near the void volume and are retained in the stacking gel of standard SDS-PAGE (lanes 1–2). (**C**) Eluted fractions from urea-soluble extracts of α-synuclein wild-type transgenic mice reveal a monomeric α-synuclein band (lane 4) in addition to an intense absorbance peak near the void volume. (**D**) Eluted fractions from urea-soluble extracts of α-synuclein E57K transgenic mice also had an intense absorbance peak near the void volume although the oligomeric species were bigger in size than those extracted from wild-type transgenic mice (compare lanes 1–2 of **C** with lanes 1–4 of **D**). There was no evidence of a band corresponding to monomeric α-synuclein in the α-synuclein E57K transgenic urea-soluble homogenates. EV = elution volume; HMW = high molecular weight; tg = transgenic; WB = western blot; wt = wild-type.

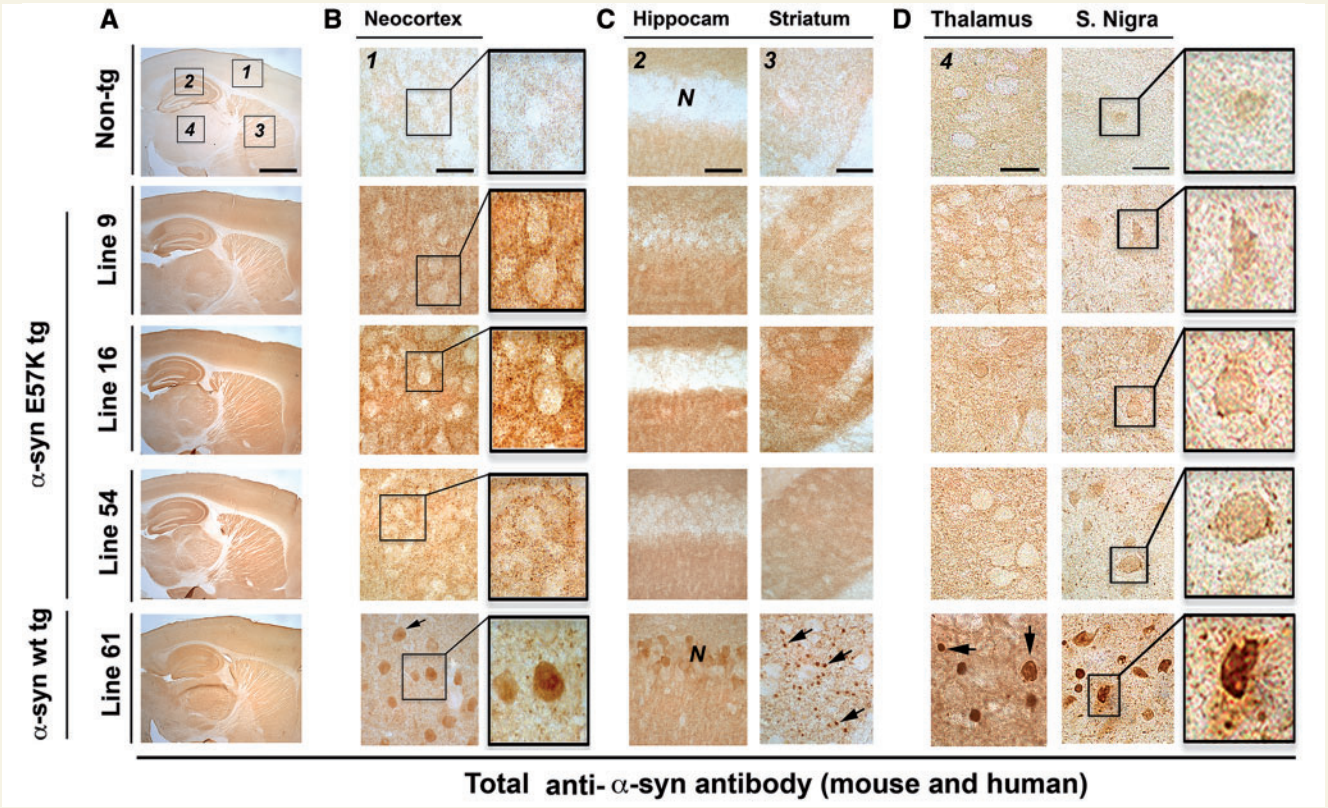

Figure 4 Comparison of the patterns of α-synuclein distribution in the brains of the α-synuclein E57K and α-synuclein wild-type transgenic mice. Vibratome sections were immunostained with the rabbit polyclonal antibody (Millipore) against full-length total α-synuclein. (**A**) Low-magnification photomicrographs of regions of interest, including the neocortex (1), hippocampus (2), striatum (3) and (4) thalamus in the non-transgenic α-synuclein E57K and α-synuclein wild-type transgenic mice. (**B**) Staining against α-synuclein was present in the neuropil of the neocortex in Lines 9 and 16, and to a lesser extent in Line 54, whereas in the α-synuclein wild-type transgenic Line 61 mouse model, α-synuclein immunoreactivity was present in the neuropil and neuronal cell bodies (arrow). The inset box illustrates a detailed area at higher magnification. (**C**) Immunoreactive α-synuclein punctae were also present in the neuropil of the hippocampus and striatum in Lines 9 and 16, and to a lesser extent in Line 54, whereas in the α-synuclein wild-type transgenic Line 61 mice, α-synuclein immunostaining was also present in neuronal cell bodies (N) and dystrophic neurites (arrows). (**D**) α-Synuclein was present in the neuropil of the thalamus in Lines 9 and 16, and to a lesser extent in Line 54, and occasionally in the cell bodies in the substantia nigra pars compacta (insets) whereas in the α-synuclein wild-type transgenic Line 61 tissue, α-synuclein immunostaining was present in the neuropil and dystrophic neurites. In the substantia nigra pars compacta, α-synuclein accumulated in the neuronal cell bodies (arrows). For analysis, six non-transgenic, $n = 6$ α-synuclein E57K transgenic mice from each line and six α-synuclein wild-type transgenic Line 61 mice (8–10 months old) were used. Scale bars: **A** = 150 μm; **B** = 25 μm; **C** = 50; **D** = 25 μm.

consistent with the distribution of the endogenous murine α-synuclein (Fig. 4A–D). Transgenic α-synuclein E57K mice from Lines 9 and 16 displayed intense immunoreactivity within the neuropil in the neocortex (Fig. 4A and B), limbic system (Fig. 4A and C), basal ganglia (Fig. 4A and C), thalamus and substantia nigra pars compacta (Fig. 4A and D), whereas α-synuclein was not observed in most neuronal cells bodies in any of the α-synuclein E57K lines (Fig. 4B and C), although occasionally there were α-synuclein-positive neuronal cell bodies in the substantia nigra (Fig. 4C). Consistent with the immunoblot analysis, mice from Line 54 showed a similar distribution of α-synuclein, but to a lesser extent than Lines 9 and 16 (Fig. 4). In contrast, tissue from Line 61 over-expressing α-synuclein wild-type mice (Rockenstein *et al.*, 2002) showed intense immunoreactivity that was detected in the neuropil and in neuronal cell bodies, in some instances mimicking intracellular inclusions (Fig. 4B–D arrows).

To further investigate the presence and distribution of α-synuclein aggregates in the brains of the α-synuclein E57K mice, immunocytochemical analysis was performed in sections pretreated with proteinase K. Previous studies have shown that α-synuclein aggregates are proteinase K resistant (Takeda *et al.*, 1998; Kahle *et al.*, 2001). As expected, in untreated (proteinase K−) sections from the α-synuclein E57K mice, most α-synuclein immunoreactivity was present in the presynaptic terminals (Fig. 5A), whereas in the α-synuclein wild-type mice, α-synuclein was detected in the neuropil and neuronal cell bodies (Fig. 5A). After treatment (proteinase K+), α-synuclein immunoreactivity in the synapses of the non-transgenic and α-synuclein mice was considerably reduced; however, in the higher-expressing (Lines 9 and 16) α-synuclein E57K mice we noticed the appearance of abundant, enlarged and tortuous neurites, but not in the low expressing line (Line 54; Fig 5A). Similarly, in the α-synuclein

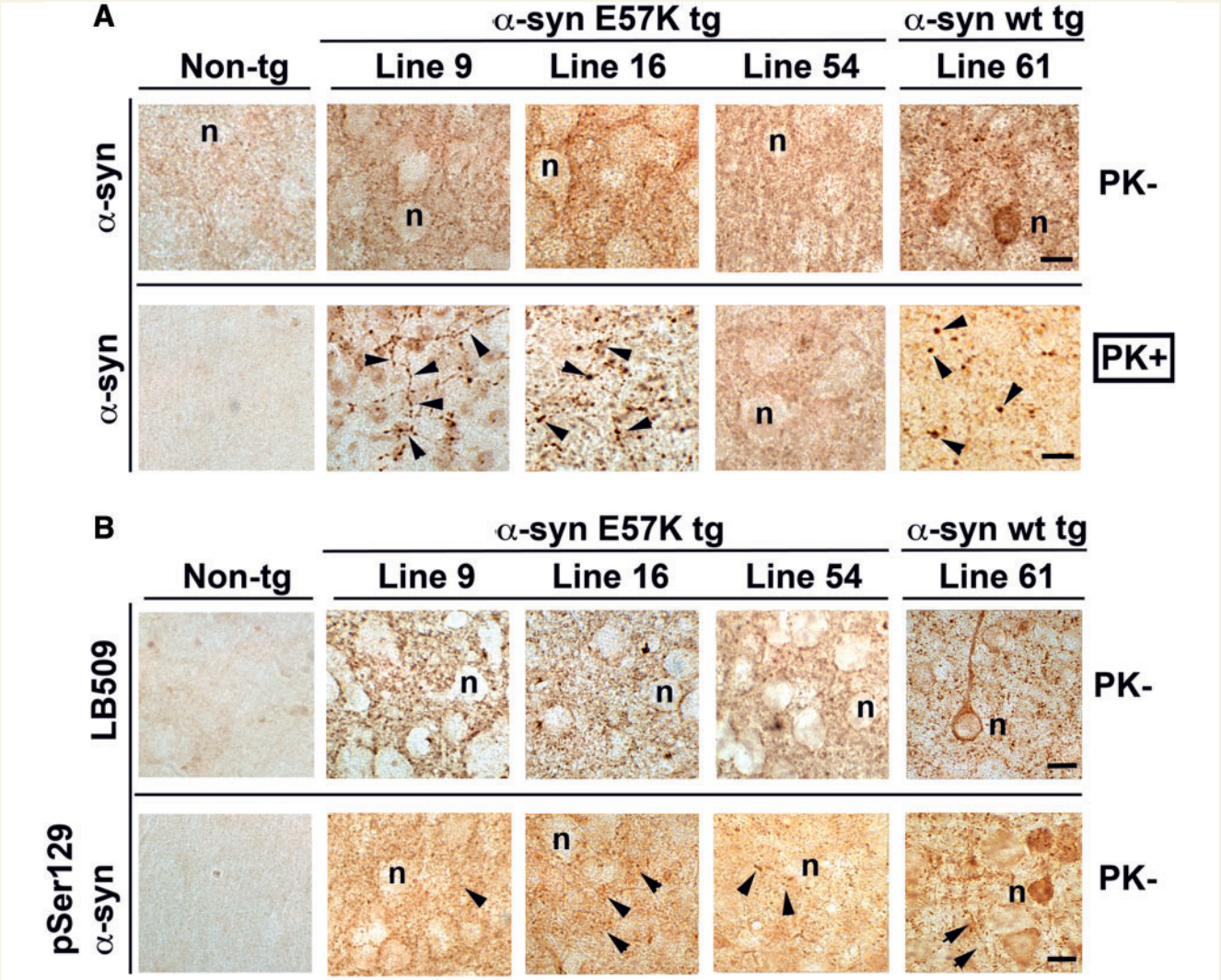

Figure 5 Accumulation of proteinase K-resistant α-synuclein in the α-synuclein E57K transgenic mice. (**A**) Representative photomicrographs (frontal cortex) of brain sections from non-transgenic and α-synuclein transgenic mice immunostained with the α-synuclein polyclonal antibody (Millipore) without proteinase K (PK−, *top*) and with proteinase K (PK+, *bottom*) treatment. In the proteinase K-treated tissue from non-transgenic and α-synuclein transgenic mice, the antibody stained the neuropil as well as the neurons (n) in the Line 61 mice. The proteinase K+ treatment eliminated most of the neuropil immunostaining in the non-transgenic mice, while at the same time revealing α-synuclein in axons (arrowheads), as well as in dystrophic neurites in the neuropil of the α-synuclein E57K transgenic Lines 9 and 16 and the α-synuclein wild-type transgenic Line 61 mice. (**B**) Patterns of LB509 (pathological α-synuclein, *top*) immunostaining in the neocortex of the non-transgenic and α-synuclein transgenic mice. The non-transgenic mice did not immunoreact with the LB509 antibody, whereas in the α-synuclein E57K transgenic mice, α-synuclein immunostaining was present in the neuropil. The α-synuclein wild-type transgenic Line 61 mice displayed α-synuclein accumulation in the neuron cell body (n) and neuropil. Patterns of p129S α-synuclein immunostaining in the neocortex of the non-transgenic and α-synuclein transgenic (*bottom*) indicated that the non-transgenic mice showed no labelling with the pSer129 antibody whereas the α-synuclein E57K transgenic mice showed α-synuclein immunostaining in the neuropil (arrowheads). The α-synuclein wild-type transgenic Line 61 mice presented α-synuclein accumulation in the neuron cell body (n) and neuropil. Scale bar = 10 μm. Four non-transgenic and four α-synuclein E57K transgenic mice (8–10 months old) from each line were used. Tg = transgenic; wt = wild-type.

wild-type mice, proteinase K pretreatment resulted in the appearance of α-synuclein-positive granular structures in the neuropil, whereas the neuronal and synaptic α-synuclein labelling was reduced (Fig. 5A). The proteinase K-resistant α-synuclein neurites were most abundant in the neocortex (Fig. 5A), in the hippocampal molecular layer and lacunosum, and in the basal ganglia and substantia nigra (not shown). In agreement with these findings, analysis with the LB509 antibody, which could detect pathological as well as other types of human α-synuclein (Jakes *et al.*, 1999), showed the presence of abundant immunoreactive granular structures in the neuropil of the α-synuclein E57K mice (Fig. 5B). In the α-synuclein wild-type mice, LB509 reacted with the neurites in the neuropil, as well as with the neuronal cell bodies (Fig. 5B). Similarly, immunostaining with an antibody against phosphorylated α-synuclein (Ser129) showed the presence of abnormal immunoreactive neurites in the higher-expressing α-synuclein

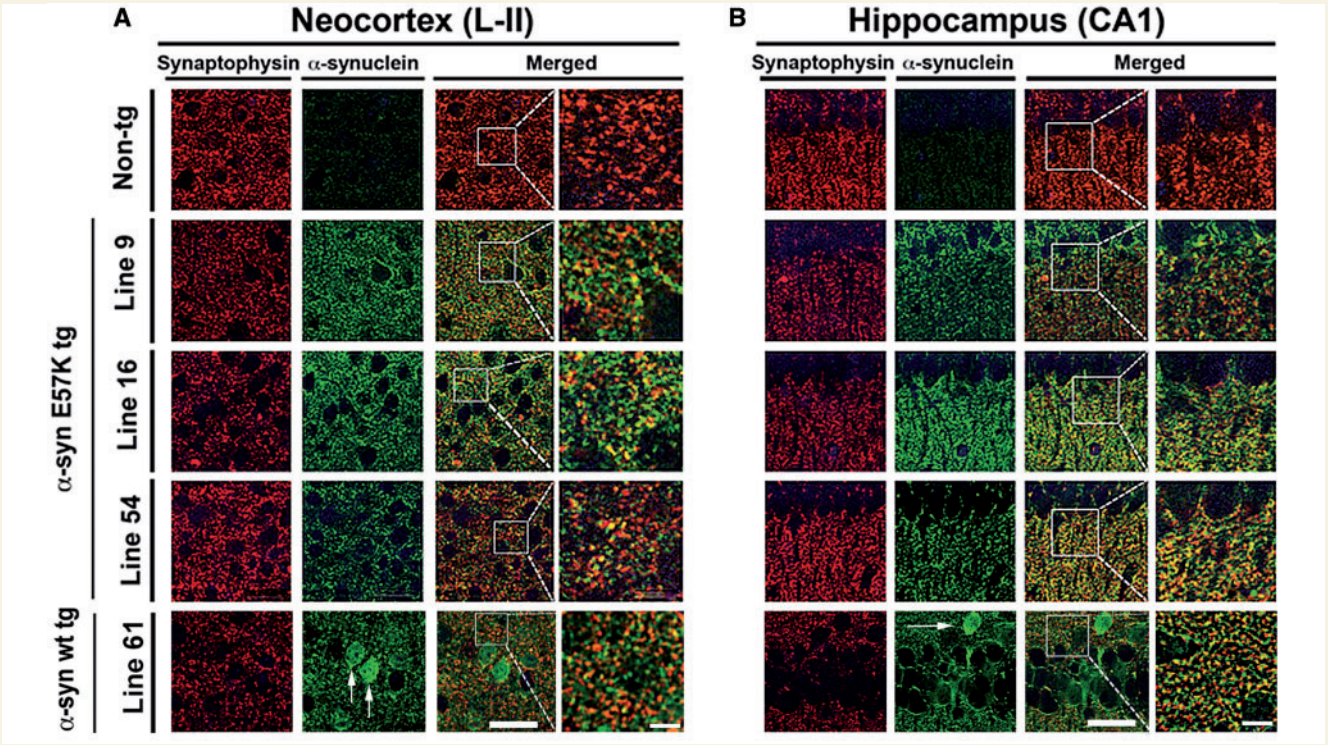

Figure 6 Immunocytochemical analysis of the synaptic co-localization between synaptophysin and α-synuclein in the α-synuclein E57K and α-synuclein wild-type transgenic mice. Sections were double-labelled with antibodies against synaptophysin (SY38, red channel) and human α-synuclein (SY211, green channel) and imaged with the laser scanning confocal microscope. (**A**) Comparison of the patterns of co-localization between synaptophysin and α-synuclein in layer II of the neocortex across all transgenic mouse lines. The transgenic lines displayed extensive co-localization between the two synaptic markers. The split image in the column to the left (red) is synaptophysin, in the centre is human α-synuclein and to the right is the two channels merged. The box represents the magnified merged image. (**B**) Comparison of the patterns of co-localization in the CA1 region of the hippocampus across the α-synuclein E57K and α-synuclein wild-type transgenic mouse lines. All transgenic lines displayed extensive co-localization between the two synaptic markers. Six non-transgenic α-synuclein E57K transgenic mice from each line and six α-synuclein wild-type transgenic Line 61 mice (8–10 months old) were used for analysis. Scale bars in the single channel images = 25 μm; 5 μm in the enlarged merged images. Tg = transgenic; wt = wild-type.

E57K mice (Fig. 5B). In the α-synuclein wild-type mice, the pSer129 antibody reacted with the neurites as well as with the neuronal cell bodies (Fig. 5B).

To analyse the distribution of the transgenic human α-syn, immunofluorescent and confocal analysis was performed with the SYN211 antibody. Using confocal microscopy we found close co-localization between human α-synuclein (SYN211) and synaptophysin in the neocortex (Fig. 6A), hippocampus (Fig. 6B) and other brain regions (not shown) in all three lines of α-synuclein E57K mice, as well as in the α-synuclein wild-type expressing Line 61, indicating the accumulation of α-synuclein in the synapse. However in the latter mouse line, α-synuclein also accumulated in the neuronal cell bodies (Fig. 6).

Accumulation of oligomer-prone α-synuclein results in synaptic pathology and reduced vesicles

To determine if the accumulation of oligomerization prone α-synuclein E57K in the synapses led to neurodegenerative pathology, immunohistochemical analysis was performed (Fig. 7). As we were interested in the chronic effects of a more global accumulation of α-synuclein accumulation in brain regions relevant to dementia with Lewy bodies and Parkinson's disease with dementia, analyses hereafter were performed in the frontal cortex and hippocampus. Confocal analysis of synaptic terminals with an antibody against synaptophysin showed a significant 20–40% loss in the frontal cortex in the higher-expressing Lines 9 and 16, as well as Line 61, but not in Line 54 (Fig. 7A and C). In the hippocampus there was a similar loss in Lines 16 and 61, but not Lines 9 or 54 (Fig. 7C). Likewise, analysis of dendrites with an antibody against MAP2 displayed a significant 20–40% loss in the frontal cortex of the higher-expressing Lines 9 and 16, as well as Line 61, but not in Line 54 (Fig. 7C). In the CA1-CA3 regions of the hippocampus, there was a significant reduction across all lines (Fig. 7B and C).

As the higher-expressing α-synuclein E57K mice displayed synaptic accumulation of α-synuclein accompanied by decreased synaptophysin and MAP2 immunoreactivity, and as we have previously shown that accumulation of α-synuclein oligomers impairs the transport of synaptic proteins (Scott *et al.*, 2010), immunoblot analysis was performed using fronto-temporal cortex. Levels of synaptophysin showed a trend toward a reduction in Line 9 as well as Line 61 and were significantly reduced by 20% in Line 16 (Fig. 8A and B). In Lines 9 and 16, as well as Line 61, levels of synapsin 1 were significantly

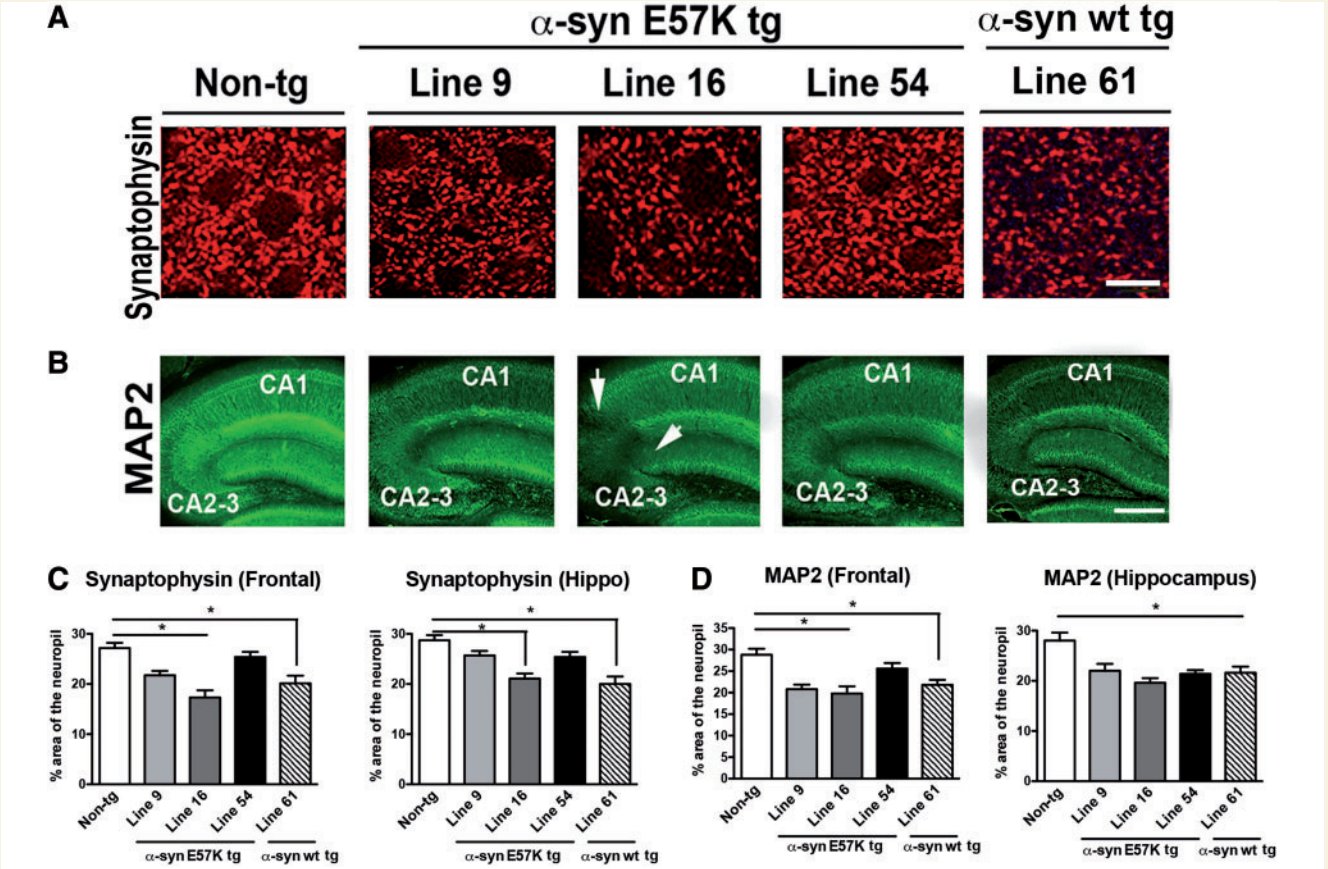

Figure 7 Analysis of synapto-dendritic loss in the frontal cortex and hippocampus from α-synuclein E57K and α-synuclein wild-type transgenic mice. Sections were immunolabelled with antibodies against synaptophysin (SY38) and MAP2, and imaged with a laser scanning confocal microscope. (**A**) Representative photomicrographs of the presynaptic terminals (SY38) and (**B**) dendrites (MAP2) in the hippocampus. Arrows indicate areas of dendritic loss in Line 16 in the CA2-3 region. Analysis was expressed as per cent area of the neuropil. (**C**) Compared with non-transgenic controls, α-synuclein E57K transgenic mice from Lines 9 and 16, as well as α-synuclein wild-type Line 61, displayed a significant reduction in synapotophysin in the frontal cortex, whereas line 54 (lower-expressing) was comparable non-transgenic littermates. In the hippocampus (hippo), synaptophysin was reduced in α-synuclein E57K Line 16 and the α-synuclein wild-type Line 61. (**D**) MAP2 was reduced in the frontal cortex in α-synuclein E57K Lines 9 and 16, as well as α-synuclein wild-type Line 61, but not in α-synuclein E57K Line 54. In the hippocampus, MAP2 was reduced across all transgenic lines. $n = 8$ mice per group, age 8–10 months. $^*P < 0.05$ when compared with non-transgenic using one-way ANOVA with Dunnet *post hoc* test. Scale bar = 10 μm for top row, 40 μm for the second row. Tg = transgenic; wt = wild-type.

reduced by 30–50%, and levels of RIMS3 were significantly reduced by 55% in Line 16 (Fig. 8A and B). In contrast, levels of SNAP25 were not altered when compared to non-transgenic controls (Fig. 8A and B). Further analysis of the frontal cortex using double-labelling and confocal microscopy confirmed that the proportion of synaptophysin (SY38) immunoreactive terminals containing synapsin 1 was significantly decreased by 50–60% in the higher-expressing Lines 9 and 16, as well as the α-synuclein wild-type Line 61 (Fig. 8C and D), compared with non-transgenic controls and the lower-expressing Line 54.

To further investigate alterations in the synaptic terminals of the α-synuclein E57K mice, ultrastructural analysis was performed using transmission electron microscopy (TEM) and immunogold. Compared to non-transgenic controls (Fig. 9A), mice from higher-expressing α-synuclein E57K Lines 9 and 16, as well as α-synuclein wild-type Line 61, showed synaptic accumulation of electro-dense bodies. In addition, Lines 9, 16 and 61 showed a significant reduction in the numbers of synaptic vesicles in the nerve terminals (Fig. 9A). To ascertain if these ultrastructural alterations in the presynaptic terminals were associated with the accumulation of α-synuclein, immunogold analysis was performed using an antibody against pathological α-synuclein (LB509) (Fig. 9C and D). In the higher-expressing α-synuclein E57K and α-synuclein wild-type Line 61 mice, abundant gold particles were detected in the enlarged nerve terminals that displayed distended vesicles (Fig. 9C and D), compared with the non-transgenic controls (Fig. 9C). Taken together these results are consistent with the double-labelling and confocal studies, indicating that accumulation of oligomer-prone α-synuclein E57K disturbs synaptic vesicles. Similar effects were observed in α-synuclein wild-type Line 61

Neuronal loss pathology in α-synuclein E57K mice

To determine if the alternations in the synapses (Figs 7–9) had an effect on neuron cell bodies, stereological assessment of NeuN-

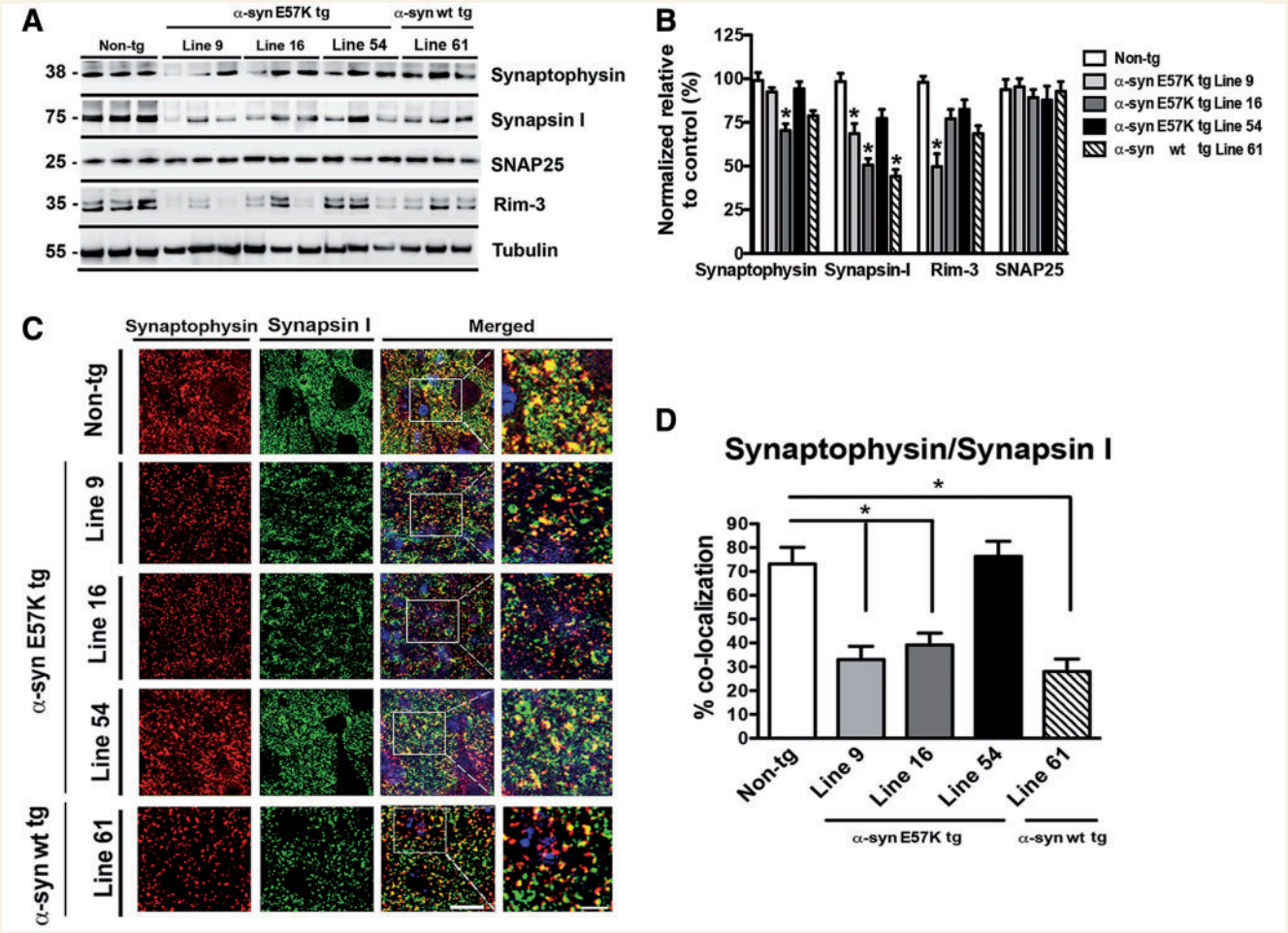

Figure 8 Analysis of alterations in synaptic protein markers in the α-synuclein E57K and α-synuclein wild-type transgenic mice. (**A**) Brain tissues from the fronto-temporal cortex were homogenized and separated into particulate and cytosolic fractions. The particulate fraction was used for the immunoblot analysis. Representative immunoblot analysis of antibodies against synaptophysin, synapsin 1, SNAP25 and RIM-3 comparing non-transgenic mice to the different α-synuclein transgenic lines. (**B**) Analysis of integrated pixels of the immunoblot shows a decrease in the synaptic protein synaptophysin in α-synuclein E57K Line 9, and RIM-3. In α-synuclein E57K transgenic mice from synapsin 1, levels were also significantly decreased in Lines 9, 16 and 61, but not in Line 54. (**C**) Sections were triple-labelled with antibodies against synaptophysin (SY38, red channel), synapsin 1 (green channel), and DAPI (blue channel) and imaged with the laser scanning confocal microscope. The right column represents the zoomed merged image (inset). The yellow dots represent co-localization between the two synaptic markers. (**D**) Image analysis of confocal images to estimate the percentage of synaptophysin terminals containing synapsin 1 immunostaining. Compared with non-transgenic controls, the higher-expressing α-synuclein E57K transgenic mice from Lines 9 and 16 showed a significant reduction in co-localization, as did the α-synuclein wild-type transgenic mice. No alterations were observed in mice from Line 54 (lower expressing). $n = 8$ mice per group, age 8–10 months. $^*P < 0.05$ when compared with non-transgenic by one-way ANOVA with Dunnet *post hoc* analysis. Scale bars are 10 μm in the merged image and 5 μm in the enlarged panels. Tg = transgenic; wt = wild-type.

positive cells was determined in the frontal cortex, hippocampus, and basal ganglia (Fig. 10A and B). In the frontal cortex, only the α-synuclein E57K Line 16 had a significant reduction in the number of neurons compared with non-transgenic controls, whereas in the hippocampus, there was a significant loss across α-synuclein E57K and α-synuclein wild-type mice (Fig. 10B). There were no changes in the neuronal population in the striatum (Fig. 10B). These neuronal alterations were accompanied by a significant increase in GFAP immunoreactivity in the neocortex and hippocampus in all mutant α-synuclein lines, as well as in Line 61 (Fig. 10C).

Behavioural deficits are exacerbated in α-synuclein E57K compared to α-synuclein wild-type mice

To evaluate the functional effects of the accumulation of the oligomer-prone α-synuclein E57K, analysis was performed using a context-dependent open field test in young and older α-synuclein E57K mice and compared with non-transgenic and α-synuclein wild-type mice. As most of the neuropathological analysis was performed in the frontal cortex and hippocampus, behavioural assessment of memory

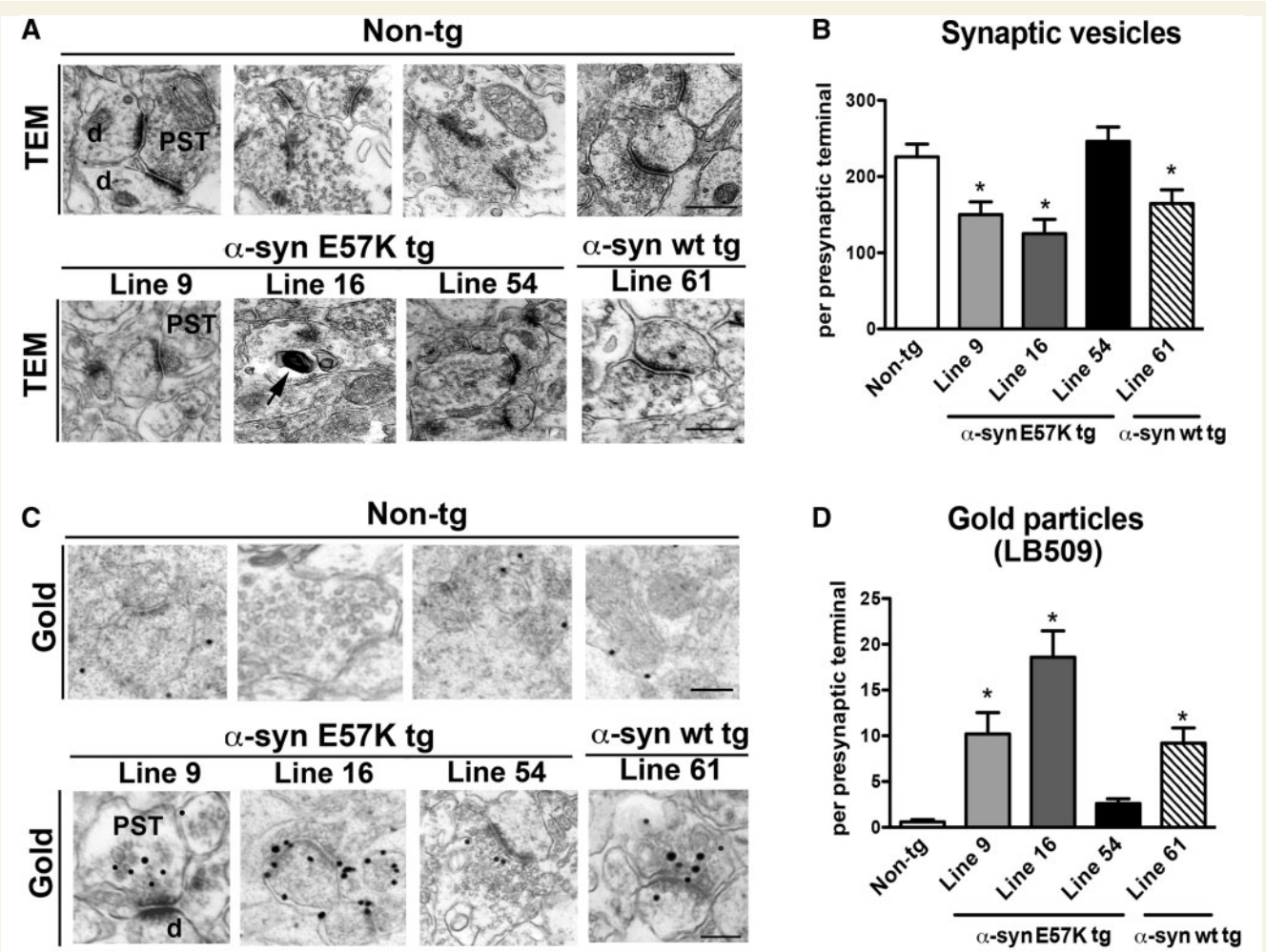

Figure 9 Ultrastructural and immunogold analyses of the synaptic terminals in the α-synuclein E57K and α-synuclein wild-type transgenic mice. Vibratome sections were post-fixed with glutaraldehyde and embedded in Epon® araldite, and ultra-thin sections from the neocortex were prepared for transmitted electron microscopy (TEM) and immunogold analysis. (**A**) Representative electron micrographs from the neuropil of non-transgenic mice displaying normal characteristics for presynaptic terminals (PST), post-synaptic densities, and dendrites (d). In the neuropil of the higher expressing α-synuclein E57K transgenic Lines 9 and 16, and in the α-synuclein wild-type Line 61, the synapses showed depletion of vesicles in the nerve terminals. Electrodense bodies were seen in Line 16 (arrow). (**B**) Image analysis of serial micrographs to estimate the numbers of synaptic vesicles per terminal. Compared with non-transgenic controls, the higher-expressing α-synuclein E57K transgenic mouse Lines 9 and 16, and α-synuclein wild-type Line 61, showed a significant reduction in the number of vesicles. No alterations were observed in mice from Line 54 (lower expressing). (**C**) Representative electron micrographs from the neuropil of non-transgenic mice immunostained with the LB509 antibody against pathological α-synuclein. Only a few scattered gold particles were detected in the neuropil. In the neuropil of the α-synuclein E57K transgenic and α-synuclein wild-type lines, the synapses showed abundant gold particles clustering at the nerve terminals and mitochondria. (**D**) Image analysis of serial micrographs to estimate the numbers of gold particles (LB509 reactive) per terminal. Compared with non-transgenic controls the higher-expressing α-synuclein E57K transgenic mouse Lines 9 and 16 showed a significant increase, as did α-synuclein wild-type Line 61. To a lesser extent, mice from Line 54 (lower expressing) also displayed accumulation of gold particles in synapses. $n = 4$ mice per group, age 8–10 months. $^*P < 0.05$ when compared with non-transgenic using one-way ANOVA with Dunnet *post hoc* test. Scale bar = 1 μm for **A** and **B**; 0.5 μm for **D** and **E**. Tg = transgenic; wt = wild-type.

acquisition was performed. At the younger age, there was a significant interaction between time and genotype ($P < 0.0001$), in addition to a significant effect as a result of time ($P = 0.0003$), as evaluated using a two-way ANOVA with repeated measures. Moreover, the young (3–4 months old) non-transgenic and lower-expressing α-synuclein E57K Line 54 mice showed habituation to the novel environment, as evidenced by decreased activity on the last day of testing (Fig. 11A). In contrast, α-synuclein E57K Lines 9 and 16 mice displayed trends toward continued high activity and failure to habituate (no learning; Fig. 11A). These trends were reiterated between genotypes when compared to the non-transgenic mice during the fourth trial (Fig. 11B). At the older age, there was a significant interaction between time and genotype ($P = 0.0011$), in addition to a significant effect because of time ($P = 0.0003$) and genotype ($P = 0.0135$), as evaluated using a two-way ANOVA with repeated measures (Fig. 11C). Both the older, 8–10 month non-transgenic and

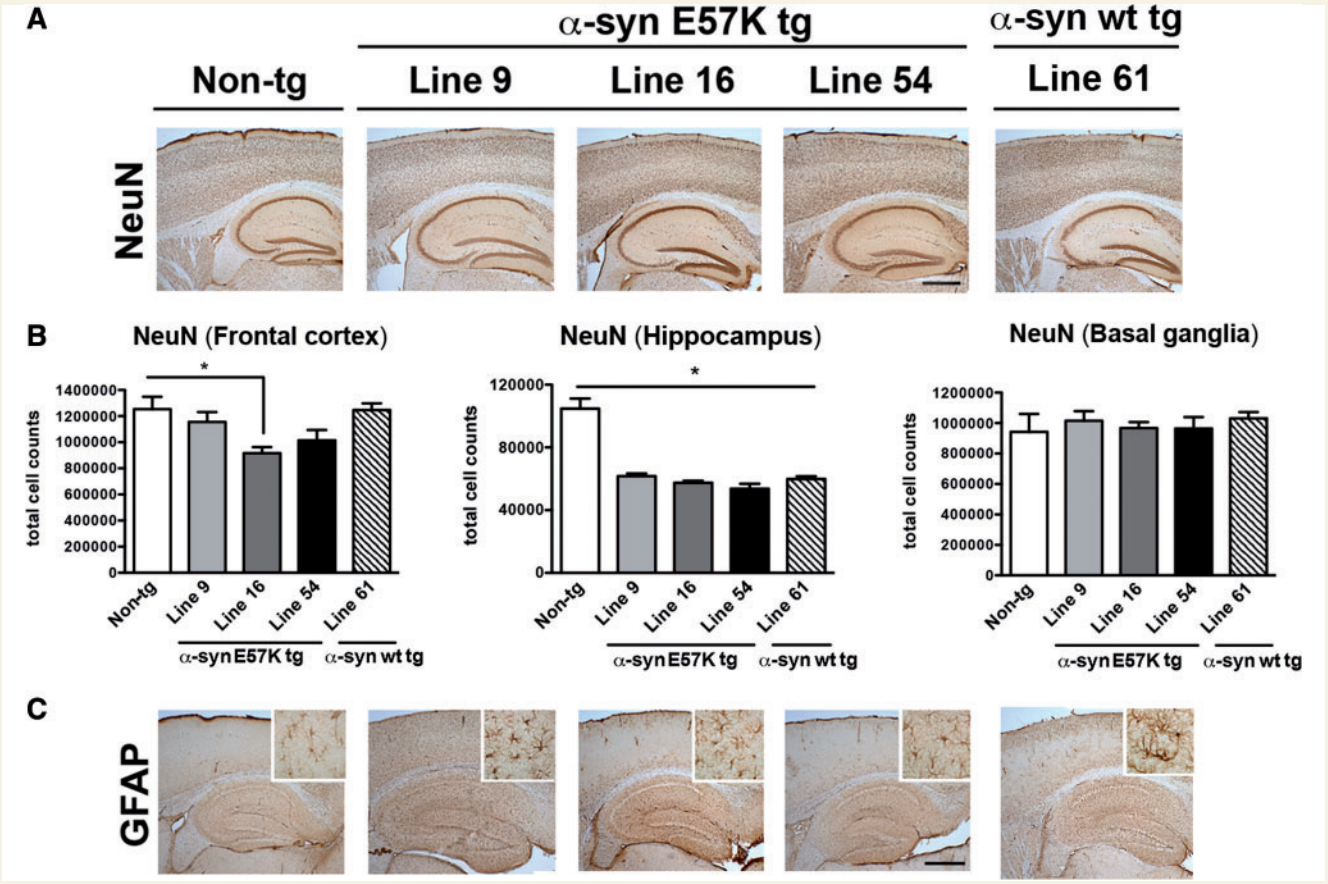

Figure 10 Analysis of neurons and astroglial cells in the α-synuclein E57K and α-synuclein wild-type transgenic mice. Sections were immunolabelled with antibodies against NeuN and GFAP and imaged with a digital bright field microscope. (**A**) Representative photomicrographs of the neocortex and from non-transgenic α-synuclein E57K, and α-synuclein wild-type Line 61 transgenic mice displaying neuronal populations (NeuN). (**B**) Stereological assessment of the number of neurons in the frontal cortex, pyramidal cell layer of the CA3 of the hippocampus, and striatum was performed. In the frontal cortex, only α-synuclein E57K Line 16 showed a significant decrease in the number of NeuN-immunoreactive cells compared to non-transgenic mice. In the hippocampus, all transgenic mouse lines showed a significant reduction in NeuN-positive cells, whereas the striatum was unaffected. (**C**) Astrogliosis (GFAP, inset represents higher magnification) was apparent by visual inspection in α-synuclein E57K Lines 9 and 16, as well as in α-synuclein wild-type Line 61, and to a lesser extent in α-synuclein E57K Line 54. Scale bars: **A** and **C** = 100 μm. $^*P < 0.05$ when compared with non-transgenic using one-way ANOVA with Dunnet *post hoc* test. Tg = transgenic; wt = wild-type.

lower expressing α-synuclein E57K Line 54 mice showed habituation and thus learning, whereas in the α-synuclein E57K Line 9 there was a significant difference in activity ($P < 0.0001$; two-way ANOVA followed by Bonferroni multiple comparisons *post hoc* test). When comparing genotypes to the non-transgenic controls during the fourth trial, α-synuclein E57K Lines 9 and 16 and α-synuclein wild-type Line 61 were significantly different and failed to habituate to the environment (forgetting) (Fig. 11D).

Discussion

In the present study, we investigated the contribution of long-term accumulation of α-synuclein oligomers to early synaptic toxicity in mice expressing low and high levels of oligomerization-prone α-synuclein E57K compared to α-synuclein wild-type (Line 61) and non-transgenic mice. We found that, with this artificial mutation, α-synuclein accumulates primarily in the synapses, leading to early reduction in synaptophysin- and MAP2-immunoreactivity and alterations associated with impaired localization of synapsin 1 to the terminals. Loss of synaptic markers could indicate synaptic degeneration or reduced localization or expression of the protein as a result of α-synuclein accumulation in the synapse. We previously showed that the α-synuclein E57K mutant tended toward oligomerization rather than fibril formation, and direct lentiviral vector injection of α-synuclein E57K resulted in greater dopaminergic neuronal loss compared with other mutants and to wild-type α-synuclein (Winner *et al.*, 2011). The tyrosine hydroxylase deficits within the E57K viral vector model were similar to those observed with naturally occurring mutations such as E46K. The present study is different from this earlier study in that we investigated the effects of more widespread and chronic expression of oligomer-prone α-synuclein on early synaptic pathology rather than the local acute effects on a restricted circuitry, as in the experiments involving the lentiviral injections.

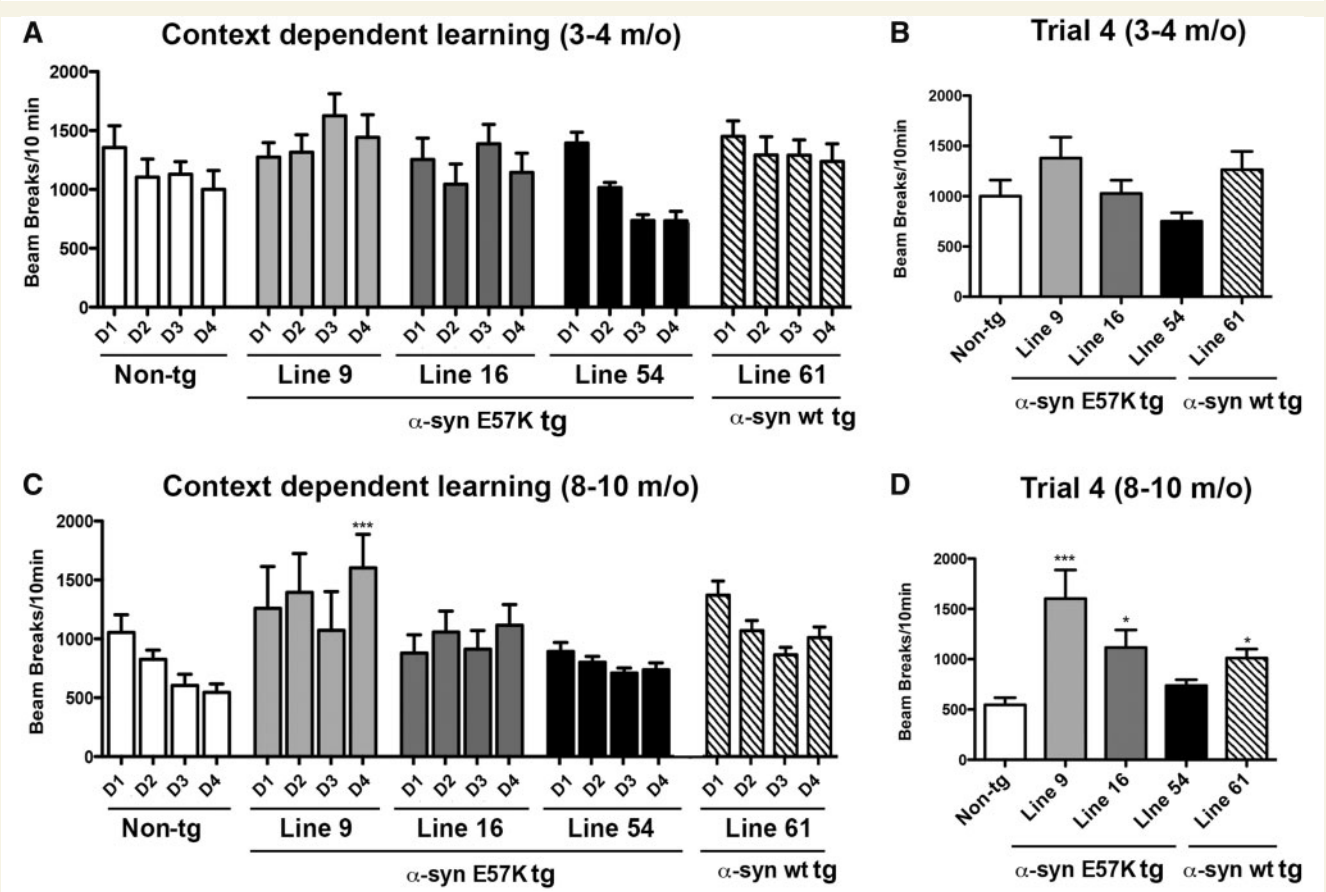

Figure 11 Memory alterations in the α-synuclein E57K and α-synuclein wild-type transgenic mice. Mice were evaluated for context-dependent learning in an open field area first at 3–4 months of age and then at 8–10 months in a Kinder SmartFrame Cage Rack Station activity monitor system. (**A**) At 3–4 months of age, non-transgenic controls and α-synuclein E57K transgenic Line 54 (lower-expressing) mice had reduced levels of activity over time as they became more familiar with the environment in the cage. The α-synuclein E57K transgenic mice from Lines 9 and 16 and the α-synuclein wild-type Line 61 transgenic mice showed a similar level of activity over time. (**B**) Evaluation of the fourth day of assessment compared to non-transgenic mice suggested trends toward dishabituation in α-synuclein E57K Line 9 and α-synuclein wild-type Line 61 (one-way ANOVA with Dunnett's multiple comparisons *post hoc* test). (**C**) Both the older 8–10 month non-transgenic and lower-expressing α-synuclein E57K Line 54 mice showed habituation and thus learning, whereas in the α-synuclein E57K Line 9 there was a significant difference in activity ($P < 0.0001$; two-way ANOVA followed by Bonferroni multiple comparisons *post hoc* test). (**D**) When comparing genotypes to the non-transgenic controls during the fourth trial, α-synuclein E57K Lines 9 and 16 and α-synuclein wild-type Line 61 were significantly different and failed to habituate to the environment (forgetting). $n = 12$ non-tg, $n = 7$ α-synuclein E57K Line 9, $n = 8$ α-synuclein E57K Line 16, $n = 14$ α-synuclein E57K Line 54, n = 14 α-synuclein wild-type Line 61 mice per age group. $^{*}P < 0.05$; $^{***}P < 0.001$ when compared with non-transgenic by one-way ANOVA with Dunnet *post hoc* analysis. Tg = transgenic; wt = wild-type; m/o = month old.

A recent study used AAV2 to investigate the effects of aggregation of α-synuclein (Taschenberger *et al.*, 2012) on the progression of neurodegeneration by expressing proline substitution variants with different fibrillation propensities in the rat substantia nigra. The conformational changes induced by proline substitutions slowed fibril formation, most likely by impairing α-helix formation. Although these proline substitutions (A30P/A56P/A76P) had a pathologic effect when combined in rat cortical neurons and *Caenorhabditis elegans*, formation of proteinase K-resistant α-synuclein aggregates was associated with loss of nigral dopaminergic neurons and striatal fibres. Expression of two prefibrillar, structure-based design mutants of α-synuclein (i.e. A56P and A30P/A56P/A76P) resulted in some neuronal loss in nigral dopaminergic neurons. However, only the α-synuclein variants capable of forming fibrils (wild-type/A30P) induced a sustained progressive loss of adult nigral dopaminergic neurons. These AAV-based systems had slower onset of tyrosine hydroxylase loss, depending on the promoter, between 4 and 24 weeks (St Martin *et al.*, 2007; Taschenberger *et al.*, 2012). The differences seen between models might differ in the extent and duration of prefibrillar toxicity. Burre *et al.* (2012) also introduced different proline substitutions by injecting a lentivirus construct into mouse substantia nigra. Depending on the localization of the mutation within α-synuclein, the introduction of these mutational changes by proline substitution were able to induce dopaminergic loss within the NAC region (residues 61–95) and in the familial

A30P mutation, but not in mutations between residues 31 and 59. In addition, these mutations do not have an impact on the physiological role of α-synuclein in synaptic vesicles. In contrast, in this system the familial A53T, E46K mutations also had a major increase in pathology (Burre *et al.*, 2012). We therefore concluded that proline substitutions might induce more selective toxicity. The difference between our results and those of the study by Taschenberger *et al.*, (2012) can be explained by differences in α-synuclein structure and synaptic function induced by E–K mutations (negative charge to positive charge) that either led to different forms of prefibrillar structures or had differential impact on nucleation of aggregation of α-synuclein wild-type.

As behavioural and neurodegenerative pathology was present primarily in the higher-expressing mice as compared with the lower-expressing line, this implies a dose-dependent effect. Although the mutation we used is artificial, the α-synuclein oligomers are biochemically and ultrastructurally similar to those described with α-synuclein wild-type and with familial mutants such as A53T (Lashuel *et al.*, 2002). Although the identity of toxic α-synuclein conformers and species *in vivo* are intensely investigated, it is clear from this and other studies that oligomerization plays a central role in neurodegeneration and the damage begins at the synaptic site and spreads back to the axons and neuronal cell bodies. For example, in the brains of patients with Parkinson's disease and dementia with Lewy bodies, proteinase K-resistant α-synuclein accumulates primarily at the nerve terminals, where it might affect synaptic function and axonal transport (Kahle *et al.*, 2001; Scott *et al.*, 2010). Similar proteinase K-resistant α-synuclein aggregates were detected in synapses and axons of α-synuclein E57K mice. These proteinase K-resistant α-synuclein deposits correlate with synaptic and dendritic damage in dementia with Lewy bodies/Parkinson's disease (Schulz-Schaeffer, 2010). The precise mechanisms through which α-synuclein oligomers might damage the synapse are not completely understood; however, interference with synaptic vesicle proteins (Burre *et al.*, 2010; Fortin *et al.*, 2010; Choi *et al.*, 2013), axonal transport (Scott *et al.*, 2010), calcium homeostasis (Danzer *et al.*, 2007; Reznichenko *et al.*, 2012) and mitochondrial function (Nakamura *et al.*, 2008) are involved. Consistent with the possibility that α-synuclein oligomers might impair synaptic function by interfering with the vesicles, the present study showed that the oligomer-prone α-synuclein E57K accumulated at the presynaptic site, where they might disrupt the presynaptic localization of synapsin 1, which is essential for vesicle clustering in the active zone (Shupliakov *et al.*, 2011). In addition, the synapses had fewer synaptic vesicles, which is in agreement with a previous study which showed that in the brains of patients with dementia with Lewy bodies/Parkinson's disease and in primary neuronal cultures from α-syn:GFPe transgenic mice, synapsin 1 is mislocalized, which impairs overall synaptic function and plasticity (Scott *et al.*, 2010) and results in deficient long term potentiation (Diogenes *et al.*, 2012). The mechanisms through which synaptic oligomers disrupt synaptic vesicle function are under intense investigation. A recent study showed that dopamine-induced, large α-synuclein oligomers effectively inhibit neuronal Soluble NSF Attachment Protein Receptor (SNARE)-mediated vesicle lipid mixing by preferentially binding to the SNARE protein, synaptobrevin 2 (Choi *et al.*, 2013). In addition, large α-synuclein oligomers reduced vesicular exocytosis in PC12 cells (Choi *et al.*, 2013). Another interesting synaptic protein affected by the mutant α-synuclein was RIMS3. RIMs 1-3 are effector proteins for Rab3s, synaptic GTP-binding proteins. RIMs are localized close to the active zone at the synapse, where they interact in a GTP-dependent manner with Rab3s located on synaptic vesicles (Wang *et al.*, 2000). We currently do not have direct evidence for the interaction of the α-synuclein oligomers with RIMS3 or Rab3s proteins; however, this is a potential mechanism through which α-synuclein could disrupt synaptic vesicle localization. Further investigation will be needed in the future.

α-Synuclein can associate with cell membranes, including synaptic vesicles, retrograde axonal transport vesicles, and detergent-resistant membrane-microdomains (Maroteaux *et al.*, 1988; Jensen *et al.*, 1998; Cole *et al.*, 2002; Outeiro and Lindquist, 2003; Fortin *et al.*, 2004). We therefore used different detergents (Triton™ X-100, SDS) and a chaotropic reagent (urea) to study the solubility and equilibrium of α-synuclein and its multimers at distinct neuronal structures. Consistent with our previous finding that α-synuclein oligomers are prone to form membrane-assembling multimeric aggregates (Tsigelny *et al.*, 2007), which is further increased by the 'conformation-trapped' α-synuclein E57K mutation (Winner *et al.*, 2011), we detected a specific SDS/urea-stable α-synuclein multimer in E57K transgenic mice, and in homogenates from dementia with Lewy bodies cases. Unlike α-synuclein E57K, α-synuclein wild-type oligomers dissolve mainly as an unspecific higher-molecular smear and its monomer (Kahle *et al.*, 2002; Tofaris *et al.*, 2006). The stability of the multimer suggests that the protein may be rigid, similar to other multimeric membrane proteins (le Coutre *et al.*, 1998; Hibino and Kurachi, 2007). It is possible that tight association with detergent-resistant membrane fractions such as lipid-rafts (Fortin *et al.*, 2004) or conformational changes induced by integration into the membrane stabilize the α-synuclein E57K multimer, whereas α-synuclein wild-type aggregates are less membrane-associated and therefore dissociate into multiple higher-oligomeric and monomeric species in the presence of SDS/urea mixture. This observation is supported by new evidence that amyloid and oligomeric structures display a higher tendency to disrupt lipid formations of plasma membranes (Reynolds *et al.*, 2011; Barrett *et al.*, 2012). Therefore, the aggregates formed by the α-synuclein E57K (pentameric) and α-synuclein wild-type (monomeric) lines suggest structural similarities with urea-insoluble multimeric and monomeric α-synuclein detected in dementia with Lewy body cases.

Although higher-expressing α-synuclein E57K mice displayed similar levels of synaptic degeneration and neuronal loss in the hippocampus when compared to the α-synuclein wild-type mice, they differed in that the oligomer-prone mice displayed more severe synaptic pathology, behavioural differences and neuronal loss in the frontal cortex. This finding is consistent with the concept that oligomers drive the neurodegenerative process in dementia with Lewy bodies/Parkinson's disease in a significant manner. Failure to form fibrils, as was the case in the α-synuclein E57K lines, was associated with exacerbating pathology. In the case of the α-synuclein wild-type Line 61 mice, both oligomers and fibrillar (FILA-1 immuoreactivity) α-synuclein were present, suggesting that the conversion of α-synuclein toward fibrillar

structures may attenuate the extent of the neurodegeneration and behavioural deficits.

In summary, this study supports the hypothesis that synaptic pathology, which is common to dementia with Lewy bodies and Parkinson's disease with dementia and is an early pathological consequence of α-synuclein accumulation, may be mediated by oligomeric α-synuclein interfering with the synaptic vesicles, leading to neuronal loss. Moreover, this oligomer-prone model might be useful for evaluating therapies directed at oligomer reduction.

Acknowledgements

Human control cases were supplied by the German Brain Bank and analyses done in accordance with the Ethics Committee guidelines.

Funding

This work was funded by NIH grants AG18440, AG022074, and NS044233, as well as CIRM, the Michael J. Fox Foundation, The JPB Medical Foundation, Interdisciplinary Center of Clinical Research (IZFK), and The Lookout Fund. The authors declare no competing financial interests.

References

Applegate MD, Landfield PW. Synaptic vesicle redistribution during hippocampal frequency potentiation and depression in young and aged rats. J Neurosci 1988; 8: 1096–111.

Barrett PJ, Song Y, Van Horn WD, Hustedt EJ, Schafer JM, Hadziselimovic A, et al. The amyloid precursor protein has a flexible transmembrane domain and binds cholesterol. Science 2012; 336: 1168–71.

Burre J, Sharma M, Sudhof TC. Systematic mutagenesis of alpha-synuclein reveals distinct sequence requirements for physiological and pathological activities. J Neurosci 2012; 32: 15227–42.

Burre J, Sharma M, Tsetsenis T, Buchman V, Etherton MR, Sudhof TC. Alpha-synuclein promotes SNARE-complex assembly *in vivo* and *in vitro*. Science 2010; 329: 1663–7.

Campbell BC, McLean CA, Culvenor JG, Gai WP, Blumbergs PC, Jakala P, et al. The solubility of alpha-synuclein in multiple system atrophy differs from that of dementia with Lewy bodies and Parkinson's disease. J Neurochem 2001; 76: 87–96.

Chen Y, Huang X, Zhang YW, Rockenstein E, Bu G, Golde TE, et al. Alzheimer's beta-secretase (BACE1) regulates the cAMP/PKA/CREB pathway independently of beta-amyloid. J Neurosci 2012; 32: 11390–5.

Choi BK, Choi MG, Kim JY, Yang Y, Lai Y, Kweon DH, et al. Large alpha-synuclein oligomers inhibit neuronal SNARE-mediated vesicle docking. Proc Natl Acad Sci USA 2013; 110: 4087–92.

Cole NB, Murphy DD, Grider T, Rueter S, Brasaemle D, Nussbaum RL. Lipid droplet binding and oligomerization properties of the Parkinson's disease protein alpha-synuclein. J Biol Chem 2002; 277: 6344–52.

Conway KA, Harper JD, Lansbury PT. Accelerated *in vitro* fibril formation by a mutant alpha-synuclein linked to early-onset Parkinson disease. Nat Med 1998; 4: 1318–20.

Culvenor JG, McLean CA, Cutt S, Campbell BC, Maher F, Jakala P, et al. Non-Abeta component of Alzheimer's disease amyloid (NAC) revisited. NAC and alpha-synuclein are not associated with Abeta amyloid. Am J Pathol 1999; 155: 1173–81.

Danzer KM, Haasen D, Karow AR, Moussaud S, Habeck M, Giese A, et al. Different species of alpha-synuclein oligomers induce calcium influx and seeding. J Neurosci 2007; 27: 9220–32.

Diogenes MJ, Dias RB, Rombo DM, Vicente Miranda H, Maiolino F, Guerreiro P, et al. Extracellular alpha-synuclein oligomers modulate synaptic transmission and impair LTP via NMDA-receptor activation. J Neurosci 2012; 32: 11750–62.

Fauvet B, Mbefo MK, Fares MB, Desobry C, Michael S, Ardah MT, et al. Alpha-synuclein in the central nervous system and from erythrocytes, mammalian cells and *E. coli* exists predominantly as a disordered monomer. J Biol Chem 2012; 287: 15345–64.

Fortin DL, Nemani VM, Nakamura K, Edwards RH. The behavior of alpha-synuclein in neurons. Mov Disord 2010; 25 (Suppl 1): S21–6.

Fortin DL, Troyer MD, Nakamura K, Kubo S, Anthony MD, Edwards RH. Lipid rafts mediate the synaptic localization of alpha-synuclein. J Neurosci 2004; 24: 6715–23.

Fujiwara H, Hasegawa M, Dohmae N, Kawashima A, Masliah E, Goldberg MS, et al. alpha-Synuclein is phosphorylated in synucleinopathy lesions. Nat Cell Biol 2002; 4: 160–4.

Games D, Seubert P, Rockenstein E, Patrick C, Trejo M, Ubhi K, et al. Axonopathy in an alpha-synuclein transgenic model of Lewy body disease is associated with extensive accumulation of C-terminal-truncated alpha-synuclein. Am J Pathol 2013; 182: 940–53.

Hansen LA. The Lewy body variant of Alzheimer disease. J Neural Transm Suppl 1997; 51: 83–93.

Hardy J. Genetic analysis of pathways to Parkinson disease. Neuron 2010; 68: 201–6.

Hibino H, Kurachi Y. Distinct detergent-resistant membrane microdomains (lipid rafts) respectively harvest K(+) and water transport systems in brain astroglia. Eur J Neurosci 2007; 26: 2539–55.

Hodara R, Norris EH, Giasson BI, Mishizen-Eberz AJ, Lynch DR, Lee VM, et al. Functional consequences of alpha-synuclein tyrosine nitration: diminished binding to lipid vesicles and increased fibril formation. J Biol Chem 2004; 279: 47746–53.

Iwai A, Masliah E, Yoshimoto M, Ge N, Flanagan L, de Silva HA, et al. The precursor protein of non-A beta component of Alzheimer's disease amyloid is a presynaptic protein of the central nervous system. Neuron 1995; 14: 467–75.

Jakes R, Crowther RA, Lee VM, Trojanowski JQ, Iwatsubo T, Goedert M. Eptope mapping of LB509, a monoclonal antibody directed against human alpha-synuclein. Neurosci Lett 1999; 269: 13–6.

Jensen PH, Nielsen MS, Jakes R, Dotti CG, Goedert M. Binding of alpha-synuclein to brain vesicles is abolished by familial Parkinson's disease mutation. J Biol Chem 1998; 273: 26292–4.

Kahle PJ, Neumann M, Ozmen L, Muller V, Jacobsen H, Spooren W, et al. Hyperphosphorylation and insolubility of alpha-synuclein in transgenic mouse oligodendrocytes. EMBO Rep 2002; 3: 583–8.

Kahle PJ, Neumann M, Ozmen L, Muller V, Odoy S, Okamoto N, et al. Selective insolubility of alpha-synuclein in human Lewy body diseases is recapitulated in a transgenic mouse model. Am J Pathol 2001; 159: 2215–25.

Kayed R, Head E, Thompson JL, McIntire TM, Milton SC, Cotman CW, et al. Common structure of soluble amyloid oligomers implies common mechanism of pathogenesis. Science 2003; 300: 486–9.

Lashuel HA, Petre BM, Wall J, Simon M, Nowak RJ, Walz T, et al. Alpha-synuclein, especially the Parkinson's disease-associated mutants, forms pore-like annular and tubular protofibrils. J Mol Biol 2002; 322: 1089–102.

le Coutre J, Kaback HR, Patel CK, Heginbotham L, Miller C. Fourier transform infrared spectroscopy reveals a rigid alpha-helical assembly for the tetrameric Streptomyces lividans K+ channel. Proc Natl Acad Sci USA 1998; 95: 6114–7.

Liu CW, Giasson BI, Lewis KA, Lee VM, Demartino GN, Thomas PJ. A precipitating role for truncated alpha-synuclein and the proteasome in alpha-synuclein aggregation: implications for pathogenesis of Parkinson disease. J Biol Chem 2005; 280: 22670–8.

Maroteaux L, Campanelli JT, Scheller RH. Synuclein: a neuron-specific protein localized to the nucleus and presynaptic nerve terminal. J Neurosci 1988; 8: 2804–15.

Masliah E, Rockenstein E, Mante M, Crews L, Spencer B, Adame A, et al. Passive immunization reduces behavioral and neuropathological deficits in an alpha-synuclein transgenic model of Lewy body disease. PLoS One 2011; 6: e19338.

Masliah E, Rockenstein E, Veinbergs I, Mallory M, Hashimoto M, Takeda A, et al. Dopaminergic loss and inclusion body formation in alpha-synuclein mice: implications for neurodegenerative disorders. Science 2000; 287: 1265–9.

McKeith IG, Galasko D, Kosaka K, Perry EK, Dickson DW, Hansen LA, et al. Consensus guidelines for the clinical and pathologic diagnosis of dementia with Lewy bodies (DLB): report of the consortium on DLB international workshop. Neurology 1996; 47: 1113–24.

Nakamura K, Nemani VM, Wallender EK, Kaehlcke K, Ott M, Edwards RH. Optical reporters for the conformation of alpha-synuclein reveal a specific interaction with mitochondria. J Neurosci 2008; 28: 12305–17.

Nuber S, Harmuth F, Kohl Z, Adame A, Trejo M, Schonig K, et al. A progressive dopaminergic phenotype associated with neurotoxic conversion of alpha-synuclein in BAC-transgenic rats. Brain 2013; 136 (Pt 2): 412–32.

Nuber S, Petrasch-Parwez E, Winner B, Winkler J, von Horsten S, Schmidt T, et al. Neurodegeneration and motor dysfunction in a conditional model of Parkinson's disease. J Neurosci 2008; 28: 2471–84.

Outeiro TF, Lindquist S. Yeast cells provide insight into alpha-synuclein biology and pathobiology. Science 2003; 302: 1772–5.

Overk CR, Kelley CM, Mufson EJ. Brainstem Alzheimer's-like pathology in the triple transgenic mouse model of Alzheimer's disease. Neurobiol Dis 2009; 35: 415–25.

Paleologou KE, Oueslati A, Shakked G, Rospigliosi CC, Kim HY, Lamberto GR, et al. Phosphorylation at S87 is enhanced in synucleinopathies, inhibits alpha-synuclein oligomerization, and influences synuclein-membrane interactions. J Neurosci 2010; 30: 3184–98.

Papp MI, Lantos PL. The distribution of oligodendroglial inclusions in multiple system atrophy and its relevance to clinical symptomatology. Brain 1994; 117 (Pt 2): 235–43.

Polymeropoulos MH, Lavedan C, Leroy E, Ide SE, Dehejia A, Dutra A, et al. Mutation in the alpha-synuclein gene identified in families with Parkinson's disease. Science 1997; 276: 2045–7.

Reynolds NP, Soragni A, Rabe M, Verdes D, Liverani E, Handschin S, et al. Mechanism of membrane interaction and disruption by alpha-synuclein. J Am Chem Soc 2011; 133: 19366–75.

Reznichenko L, Cheng Q, Nizar K, Gratiy SL, Saisan PA, Rockenstein EM, et al. *In vivo* alterations in calcium buffering capacity in transgenic mouse model of synucleinopathy. J Neurosci 2012; 32: 9992–8.

Rockenstein E, Mallory M, Hashimoto M, Song D, Shults CW, Lang I, et al. Differential neuropathological alterations in transgenic mice expressing alpha-synuclein from the platelet-derived growth factor and Thy-1 promoters. J Neurosci Res 2002; 68: 568–78.

Rockenstein E, Mallory M, Mante M, Sisk A, Masliaha E. Early formation of mature amyloid-beta protein deposits in a mutant APP transgenic model depends on levels of Abeta(1-42). J Neurosci Res 2001; 66: 573–82.

Rockenstein EM, McConlogue L, Tan H, Power M, Masliah E, Mucke L. Levels and alternative splicing of amyloid beta protein precursor (APP) transcripts in brains of APP transgenic mice and humans with Alzheimer's disease. J Biol Chem 1995; 270: 28257–67.

Sanchez PE, Zhu L, Verret L, Vossel KA, Orr AG, Cirrito JR, et al. Levetiracetam suppresses neuronal network dysfunction and reverses synaptic and cognitive deficits in an Alzheimer's disease model. Proc Natl Acad Sci USA 2012; 109: E2895–903.

Schindler J, Jung S, Niedner-Schatteburg G, Friauf E, Nothwang HG. Enrichment of integral membrane proteins from small amounts of brain tissue. J Neural Transm 2006; 113: 995–1013.

Schulz-Schaeffer WJ. The synaptic pathology of alpha-synuclein aggregation in dementia with Lewy bodies, Parkinson's disease and Parkinson's disease dementia. Acta Neuropathol 2010; 120: 131–43.

Scott DA, Tabarean I, Tang Y, Cartier A, Masliah E, Roy S. A pathologic cascade leading to synaptic dysfunction in alpha-synuclein-induced neurodegeneration. J Neurosci 2010; 30: 8083–95.

Shupliakov O, Haucke V, Pechstein A. How synapsin I may cluster synaptic vesicles. Semin Cell Dev Biol 2011; 22: 393–9.

Spillantini MG, Schmidt ML, Lee VM, Trojanowski JQ, Jakes R, Goedert M. Alpha-synuclein in Lewy bodies. Nature 1997; 388: 839–40.

St Martin JL, Klucken J, Outeiro TF, Nguyen P, Keller-McGandy C, Cantuti-Castelvetri I, et al. Dopaminergic neuron loss and up-regulation of chaperone protein mRNA induced by targeted over-expression of alpha-synuclein in mouse substantia nigra. J Neurochem 2007; 100: 1449–57.

Sung JY, Park SM, Lee CH, Um JW, Lee HJ, Kim J, et al. Proteolytic cleavage of extracellular secreted {alpha}-synuclein via matrix metalloproteinases. J Biol Chem 2005; 280: 25216–24.

Takeda A, Hashimoto M, Mallory M, Sundsumo M, Hansen L, Sisk A, et al. Abnormal distribution of the non-Abeta component of Alzheimer's disease amyloid precursor/alpha-synuclein in Lewy body disease as revealed by proteinase K and formic acid pretreatment. Lab Invest 1998; 78: 1169–77.

Taschenberger G, Garrido M, Tereshchenko Y, Bahr M, Zweckstetter M, Kugler S. Aggregation of alphaSynuclein promotes progressive *in vivo* neurotoxicity in adult rat dopaminergic neurons. Acta Neuropathol 2012; 123: 671–83.

Tofaris GK, Garcia Reitbock P, Humby T, Lambourne SL, O'Connell M, Ghetti B, et al. Pathological changes in dopaminergic nerve cells of the substantia nigra and olfactory bulb in mice transgenic for truncated human alpha-synuclein(1-120): implications for Lewy body disorders. J Neurosci 2006; 26: 3942–50.

Tong Y, Yamaguchi H, Giaime E, Boyle S, Kopan R, Kelleher RJ 3rd, et al. Loss of leucine-rich repeat kinase 2 causes impairment of protein degradation pathways, accumulation of alpha-synuclein, and apoptotic cell death in aged mice. Proc Natl Acad Sci USA 2010; 107: 9879–84.

Tsigelny IF, Bar-On P, Sharikov Y, Crews L, Hashimoto M, Miller MA, et al. Dynamics of alpha-synuclein aggregation and inhibition of pore-like oligomer development by beta-synuclein. FEBS J 2007; 274: 1862–77.

Tsigelny IF, Sharikov Y, Wrasidlo W, Gonzalez T, Desplats PA, Crews L, et al. Role of alpha-synuclein penetration into the membrane in the mechanisms of oligomer pore formation. FEBS J 2012; 279: 1000–13.

Ubhi K, Rockenstein E, Mante M, Inglis C, Adame A, Patrick C, et al. Alpha-synuclein deficient mice are resistant to toxin-induced multiple system atrophy. Neuroreport 2010; 21: 457–62.

Uversky VN, Li J, Fink AL. Metal-triggered structural transformations, aggregation, and fibrillation of human alpha-synuclein - A possible molecular link between Parkinson's disease and heavy metal exposure. J Biol Chem 2001; 276: 44284–96.

Wakabayashi K, Yoshimoto M, Tsuji S, Takahashi H. Alpha-synuclein immunoreactivity in glial cytoplasmic inclusions in multiple system atrophy. Neurosci Lett 1998; 249: 180–2.

Wang Y, Sugita S, Sudhof TC. The RIM/NIM family of neuronal C2 domain proteins. Interactions with Rab3 and a new class of Src homology 3 domain proteins. J Biol Chem 2000; 275: 20033–44.

Weinreb PH, Zhen W, Poon AW, Conway KA, Lansbury PT Jr. NACP, a protein implicated in Alzheimer's disease and learning, is natively unfolded. Biochemistry 1996; 35: 13709–15.

Winner B, Jappelli R, Maji SK, Desplats PA, Boyer L, Aigner S, et al. *In vivo* demonstration that alpha-synuclein oligomers are toxic. Proc Natl Acad Sci USA 2011; 108: 4194–9.